5.10 Material Performance in Molten Salts

V. Ignatiev and A. Surenkov
National Research Centre, Kurchatov Institute, Moscow, Russian Federation

Abbreviations

AHTR	Advanced High-Temperature reactor cooled by molten salts
ARE	Aircraft Reactor Experiment
CNRS	Centre de la National Recherché Scientifique, France
dpa	Displacements per atom
FLIBE	Molten LiF-BeF_2 salt mixture
FLINABE	Molten LiF-NaF-BeF_2 salt mixture
Hastelloy N or INOR-8	Ni-Mo alloy developed for MSR at ORNL
HTR	High-Temperature Reactor cooled by helium
HX	Heat Exchanger
IGC	InterGranular Cracks
IHX	Intermediate Heat Exchanger
KI	Kurchatov Institute, Russia
LSFR	Liquid Salt-cooled Fast Reactor
LWR	Light Water Reactor
MA	Minor Actinides
MC	(U,Pu)C Metal Carbide fuel form
MOSART	Molten Salt Actinide Recycler & Transmuter
MOX	(U,Pu)O_2 Mixed Oxide fuel
MSBR	Molten Salt Breeder Reactor
MSFR	Molten Salt Fast Reactor
MSR	Molten Salt Reactor
MSRE	Molten Salt Reactor Experiment
MWe	Megawatts electrical
MWt	Megawatts thermal
NCL	Natural Convection Loop
NFC	Nuclear Fuel Cycle
NPP	Nuclear Power Plant
ODS	Oxide Dispersion-strengthened Steels
ORNL	Oak Ridge National Laboratory, USA
RE	Rare Earth elements
REDOX	Electrochemical reduction–oxidation
RW	Radioactive Wastes
SFR	Sodium-cooled Fast Reactor
SNF	Spent Nuclear Fuel
TRU	TRans-Uranium elements
UOX	UO_2 Uranium Oxide fuel
VHTR	Very High-Temperature Reactor

5.10.1 Introduction: Brief Review of Different Related Applications

In the last few years, there has been a significantly increased interest in the use of high-temperature molten salts as coolants and fuels in nuclear power and fuel cycle systems.[1–5] The potential utility of a fluid-fueled reactor that can operate at a high temperature, but with a low-pressure system, has been recognized for a long time. One of the attractive features of the molten-salt system is the variety of reactor types that can be considered to cover a range of applications. Molten salts offer very attractive characteristics as coolants, with respect to heat transport and heat transfer properties at high temperatures. The molten-salt system has the usual benefits attributed to fluid-fuel systems. The principal advantages over solid-fuel element systems are (1) a high negative temperature coefficient of reactivity; (2) lack of radiation damage that can limit fuel burnup; (3) the possibility of continuous fission-product removal; (4) the avoidance of the expense of fabricating new fuel elements; and (5) the possibility of adding makeup fuel as needed, which precludes the need for providing excess reactivity. Indeed, fuel can be processed in an online mode or in batches in order to retrieve fission products and then reintroduced into the reactor (fuel in liquid form during the whole cycle).

Molten fluoride salts were first developed for nuclear systems as a homogeneous fluid fuel. In this application, salt served as both fuel and primary coolant at temperatures $\leq$700 °C. Secondary coolant salts were also developed that contained no fissile and fertile materials. In the 1970s, because power cycle temperatures were limited by the existing steam system technology, the potential for use of molten salts at extreme temperatures was not fully explored. Today, much higher temperatures (>700 °C) are of interest for a number of important applications.

For 60 years, nitrate salts at lower temperatures have been used as coolants on a large industrial scale in heat transport systems in the chemical industry; thus, a large experience base exists for salt-base heat transport systems.[6–8] However, because these salts decompose at ~600 °C, highly stable salts are required at higher temperatures. Most of the research on high-temperature molten-salt coolants has focused on fluoride salts because of their chemical stability and relatively noncorrosive behavior. Chloride salts are a second option, but the technology is less well developed.[9,10] As is true for most other coolants, corrosion behavior is determined primarily by the impurities in the coolant and not the coolant itself. While large-scale testing has taken place, including the use of such salts in test reactors, there is only limited industrial experience.

In the 1950s and 1960s, the US Oak Ridge National Laboratory (ORNL) investigated molten-salt reactors (MSRs), in which the fuel was dissolved in the fluoride coolant, for aircraft nuclear propulsion and breeder reactors.[11] Two test reactors were built at ORNL: the Aircraft Reactor Experiment (ARE)[12–14] and the Molten Salt Reactor Experiment (MSRE).[15] The favorable experience gained from the 8 MWt MSRE test reactor operated from 1965 to 1969 led to the design of a 1000 MWe molten-salt breeder reactor (MSBR) with a core graphite moderator, thermal spectrum, and thorium–uranium fuel cycle.[16,17] In the MSBR design, fuel salt temperature at the core outlet was 704 °C. The research and development effort, combined with the MSRE and a large number of natural and forced convection loop tests, provided a significant basis for demonstrating the viability of the MSR concept.

Since the 1970s, with other countries, including Japan, Russia, and France, the United States placed additional emphasis on the MSR concept development.[18–22] Recent MSR developments in Russia on the 1000 MWe molten-salt actinide recycler and transmuter (MOSART)[1] and in France on the 1000 MWe nonmoderated thorium molten-salt reactor (MSFR)[4,5] address the concept of large power units with a fast neutron spectrum in the core. Compared to the MSBR, core outlet temperature is increased to 720 °C for MOSART and 750 °C for the MSFR. The first concept aims to be used as efficient burners of transuranic (TRU) waste from spent UOX and MOX light water reactor (LWR) fuel without any uranium and thorium support. The second one has a breeding capability when using the thorium fuel cycle. Studies of the fast-spectrum MSFR also indicated that good breeding ratios could be obtained, but high power densities would be required to avoid excessive fissile inventories. Adequate power densities appeared difficult to achieve without novel heat removal methods. Earlier proposals for fast-spectrum MSRs used chloride salts.[9] However, chloride salts have three major drawbacks: (1) a need for isotopically separated chlorine to avoid high-cross-section nuclides; (2) the activation product ^{36}Cl, which presents significant challenges to waste management because of its mobility in the environment; and (3) the more corrosive characteristics of chloride systems relative to fluoride systems.

Today, in addition to the different MSR systems, other advanced concepts that use the molten-salt technology are being studied, including the advanced high-temperature reactor (AHTR) and the liquid-salt-cooled fast reactor (LSFR).

The AHTR uses clean molten salts as the coolant and the same coated particle fuel encapsulated in graphite as high-temperature gas-cooled reactors, such as the very high-temperature reactor (VHTR). The fuel cycle characteristics are essentially identical to those of the VHTR. This concept was originally proposed in the 1980s by the RRC-Kurchatov Institute in Russia,[19] but most of the recent work is being conducted in the United States.[23] The AHTR is a longer-term high-temperature reactor option with potentially superior economics due to the properties of the salt coolant. Also, better heat transport characteristics of salts compared to helium enable power levels up to 4000 MWt with passive safety systems. The AHTR can be built in larger sizes or as very compact modular reactors, it operates at lower pressure, and the equipment is smaller because of the superior heat transfer capabilities of liquid-salt coolants compared to helium.

A newer concept is the LSFR, which is being investigated in the United States and France.[24] Liquid salts offer three potential advantages compared to sodium: (1) molten fluoride salts are transparent and have heat transport properties similar to those of water; however, their boiling points exceed 1200 °C; (2) smaller equipment size because of the higher volumetric heat capacity of the salts; and (3) no chemical reactions between the reactor, intermediate loop, and power cycle coolants. There is experience with this type of system because the ARE at ORNL used a sodium-cooled intermediate loop. The basic design of an LSFR is similar to that of a sodium-cooled fast reactor (SFR), except that a clean salt replaces the sodium and the reactor operates at higher temperatures with the potential for higher thermal efficiency. Molten-salt fluoride-based coolants allow fast-reactor coolant outlet temperatures to be increased from 500–550 °C (sodium) to 700–750 °C, with a corresponding increase in plant efficiency from 42% to ~50%.

To identify salts that produce acceptable 'voiding' (meaning thermal expansion) response, chlorides are also explored as salts for the LSFR, though one has to consider the ^{36}Cl production either by neutron capture on ^{35}Cl or (n, 2n) reaction on ^{37}Cl. Recent MSR developments in the United States on the 2400 MWt liquid-salt-cooled, flexible-conversion-ratio reactor address the concept with a core power density of 130 kW l^{-1} and a maximum cladding temperature of 650 °C.[25]

Based on technical considerations, LSFRs may have significantly lower capital costs than SFRs; thus, there is an incentive to examine the feasibility of an LSFR. There are fundamental challenges to this new reactor concept, such as development of high-temperature clads that are corrosion resistant in the salt environment, can operate at high temperatures, and can withstand high neutron radiation levels.

There are multiple industrial uses for high-temperature heat at temperatures from 700 to 950 °C.[2] There is a growing interest in using high-temperature reactors to supply this heat because of the increasing prices for natural gas and concerns about greenhouse gas emissions. Such applications require high-temperature heat transport systems to move heat from high-temperature nuclear reactors (gas-cooled or liquid-salt-cooled) to the customer. There are several economic incentives to develop liquid-salt heat transport systems rather than using helium for these applications: (1) the pipe cross-sections are less than one-twentieth of that of helium because of the high volumetric heat capacity of liquid salts; (2) salt systems can operate at atmospheric pressure; (3) better heat transfer characteristics of the salt reduce the size of heat exchangers; and (4) molten-salt pumps operate at much higher temperatures to provide heat in a narrow temperature interval, compared to compressors that circulate helium in a VHTR.[19] For most of these applications, the transport distances will exceed a kilometer.

Finally, it should be noted that fuel refining and reprocessing in systems using molten chlorides/fluorides and liquid metals (Bi, Zn, Cd, Pb, Sn, etc.) is a promising method to solve the actinide and fission product partitioning task for advanced fuels. These approaches are considered as basic for reprocessing metal, nitride, and MSR fuels.[2,4,17,19]

As can be seen from the considerations above, there are several potential applications of molten salts for future nuclear power. There is great flexibility in the use of molten-salt concepts for nuclear power in liquid-fuel and solid-fuel reactors, heat transfer loops, or fuel-processing units.

5.10.2 Choice of Fuel and Coolant Salts for Different Applications

Selection of salt coolant composition strongly depends on the specific design application: fluid fuel (burner or breeder), primary (LSFR or AHTR) or secondary coolant, heat transport fluid, etc. In choosing a fuel salt for a given fluid-fuel reactor design, the following criteria are applied[26]:

- Low neutron cross-section for the solvent components
- Thermal stability of the salt components
- Low vapor pressure
- Radiation stability

- Adequate solubility of fuel (including TRU waste) and fission-product components
- Adequate heat transfer and hydrodynamic properties
- Chemical compatibility with container and moderator materials
- Low fuel and processing costs

At temperatures up to 1000 °C, molten fluorides exhibit low vapor pressure ($\ll$1 atm) and relatively benign chemical reactivity with air and moisture. Molten fluorides also trap most fission products (including Cs and I) as very stable fluorides, and thus act as an additional barrier to accidental fission product release. Fluorides of metals other than U, Pu, or Th are used as diluents and to keep the melting point low enough for practical use. Consideration of nuclear properties alone leads one to prefer as diluents the fluorides of Be, Bi, ^{7}Li, Pb, Zr, Na, and Ca, in that order. Salts that contain easily reducible cations (Bi^{3+} and Pb^{2+}, see **Table 1**) were rejected because they would not be stable in nickel- or iron-base alloys of construction.

Three basic salt systems (see **Table 2**)[27–33] exhibit usefully low melting points (between 315 and 565 °C) and also have the potential for neutronic viability and material compatibility with alloys: (1) alkali fluoride salts, (2) ZrF_4-containing salts, and (3) BeF_2-containing salts. An inspection of the behavior of the phase diagrams for these systems reveals a considerable range of compositions in which the salt will be completely molten with concentrations of UF_4 or $ThF_4 > 10$ mol% at 500 °C and >20 mol% at 560 °C.[27] Trivalent plutonium and minor actinides are the only stable species in the various molten fluoride salts. Tetravalent plutonium could transiently exist if the salt redox potential is high enough. Solubility of PuF_4 by analogy of ZrF_4, UF_4, and ThF_4 should be relatively high. But for practical purposes (stability of potential container material), the salt redox potential should be low enough and correspond to the stability area of Pu (III). PuF_3 solubility is maximum in pure LiF, NaF, or KF and decreases with the addition of BeF_2 and ThF_4.[28–33] The solubility decrease is more for BeF_2 addition, because PuF_3 is not soluble in pure BeF_2. As can be seen from **Table 2** (column 1), the LiF–PuF_3 system is characterized by a eutectic point with 20 mol% of PuF_3 at 743 °C.[28] The calculated solubility of PuF_3 in the matrix of LiF–NaF–KF (43.9–14.2–41.9) at $T = 600$ °C has been found to be 19.3 mol%.[5] Adequate solubility of PuF_3 at 600 °C in burner (>2 mol%) and breeder fast-spectrum concepts (3–4 mol%) can also be achieved using ^{7}LiF–(NaF)–BeF_2 (column 3) and LiF–(BeF_2)–ThF_4 (column 4) systems solvent (see **Table 2**), respectively. The lanthanide trifluorides are also only moderately soluble in BeF_2- and ThF_4-containing mixtures. If more than one such trifluoride (including UF_3) is present, they crystallize to form a solid, made up of all the trifluorides, on cooling of the saturated melt so that, in effect, all the LnF_3 and AnF_3 act essentially as a single element. If so, the total (An + Ln) trifluorides in the end-of-life reactor might possibly exceed their combined solubility.

Melts of these fluorides have satisfactory values of heat capacity, thermal conductivity, and viscosity over a temperature range of 550–1000 °C and provide an efficient removal of heat when they are used as the coolant over a wide range of compositions. (See also **Chapter 3.13, Molten Salt Reactor Fuel and Coolant**). Transport properties of molten-salt coolants ensure highly efficient cooling with natural circulation; the salt–wall heat transfer coefficient is close to the same as that for water. The thermal diffusivity of the salt is 300 times smaller than that of sodium. Therefore, all other things being equal, the characteristic solidification time for a volume of the fluoride melt is 300 times longer than that of sodium.[2]

A particular disadvantage of ZrF_4-containing (more than 25 mol%) melts is its condensable vapor, which is predominantly ZrF_4.[26] The 'snow' that would form could block vent lines and cause problems in pumps that circulate the fuel. Note also that the use of Zr instead of sodium in the basic solvent will lead to

Table 1 Thermodynamic properties of fluorides

Compound (solid state)	*$-\Delta G_{f,1000}$ (kJ mol^{-1})*	*Compound (solid state)*	*$-\Delta G_{f,1000}$ (kJ mol^{-1})*
LiF	522	AlF_3	372
NaF	468	VF_2	347
KF	460	TiF_2	339
BeF_2	447	CrF_2	314
ThF_4	422	FeF_2	280
UF_3	397	HF	276
ZrF_4	393	NiF_2	230
UF_4	389	CF_4	130

Source: Novikov, V. M.; Ignatiev, V. V.; Fedulov, V. I.; Cherednikov, V. N. *Molten Salt Reactors: Perspectives and Problems*; Energoatomizdat: Moscow, USSR, 1990; Ignatiev, V. V.; Novikov, V. M.; Surenkov, A. I.; Fedulov, V. I. The state of the problem on materials as applied to molten-salt reactor: Problems and ways of solution, Preprint IAE-5678/11; Institute of Atomic Energy: Moscow, USSR, 1993; Williams, D. F.; *et al.* Assessment of candidate molten salt coolants for the advanced high-temperature reactor, ORNL/TM-2006/12; ORNL: Oak Ridge, TN, 2006.

Table 2 Molar compositions, melting temperatures (°C),[27] and solubility of plutonium trifluoride (mol%) at 600 °C in different molten fluoride salts considered as candidates for the fuel and the coolant circuits in MSR concepts

Alkali-metal fluorides	*ZrF_4-containing*	*BeF_2 containing*	*ThF_4 containing*	*Fluoroborates*
LiF–PuF_3 (80–20) 743 °C[28]				
LiF–KF (50–50) 492 °C –	LiF–ZrF_4 (51–49) 509 °C –	LiF–BeF_2 (73–27) 530 °C 2.0[32]	LiF–ThF_4 (78–22) 565 °C 4.2[29]	KF–KBF_4 (25–75) 460 °C –
LiF–RbF (44–56) 470 °C –	NaF–ZrF_4 (59.5–40.5) 500 °C 1.8[31]	LiF–NaF–BeF_2 (15–58–27) 479 °C 2.0[32,33]	LiF–BeF_2–ThF_4 (75–5–20) 560 °C 3.1[29]	RbF–$RbBF_4$ (31–69) 442 °C –
LiF–NaF–KF (46.5–11.5–42) 454 °C 19.3[5]	LiF–NaF–ZrF_4 (42–29–29) 460 °C –	LiF–BeF_2 (66–34) 458 °C 0.5[32,33]	LiF–BeF_2–ThF_4 (71–16–13) 499 °C 1.5[30]	NaF–$NaBF_4$ (8–92) 384 °C –
LiF–NaF–RbF (42–6–52) 435 °C –	LiF–NaF–ZrF_4 (26–37–37) 436 °C –	LiF–BeF_2–ZrF_4 (64.5–30.5–5) 428 °C –	LiF–BeF_2–ThF_4 (64–20–16) 460 °C 1.2[29]	
	NaF–RbF–ZrF_4 (33–24–43) 420 °C –	NaF–BeF_2 (57–43) 340 °C 0.3[32]	LiF–BeF_2–ThF_4 (47–51.5–1.5) 360 °C –	
	NaF–KF–ZF_4 (10–48–42) 385 °C –	LiF–NaF–BeF_2 (31–31–38) 315 °C 0.4[32]		
	KF–ZrF_4 (58–42) 390 °C –			

increased generation of long-lived activation products in the system. Potassium-containing salts are usually excluded from consideration as a primary coolant because of the relatively large parasitic capture cross-section of potassium. However, potassium-containing salts are commonly used in nonnuclear applications and serve as a useful frame of reference (e.g., LiF–NaF–KF). This leaves ^{7}LiF, NaF, and BeF_2 as preferred major constituents. For reasons of neutron economy at ORNL, the preferred solvents for prior Th–U MSR concepts have been LiF and BeF_2, with the lithium enriched to 99.995 in the ^{7}Li isotope. It has recently been indicated that this well-studied BeF_2-containing solvent mixture needs further consideration, in view of the current knowledge on beryllium toxicity.[4]

Unlike the MSR, AHTR and LSFR use solid fuel and a clean liquid salt as a coolant (i.e., a coolant with no dissolved fissile materials or fission products). For the MSR, a major constraint was the requirement for high solubility of fissile materials and fission products in the salt; a second was suitable for salt reprocessing. For AHTR and LSFR, these requirements do not exist. The requirements mainly include (1) a good coolant, (2) low coolant freezing points, and (3) application-specific requirements. As a result, a wider choice of fluoride salts can be considered. For a fast reactor, it is also desirable to avoid low-*Z* materials that can degrade the neutron spectrum. In all cases, binary or more complex fluoride salt mixtures are preferred because the melting points of fluoride salt mixtures are much lower than those for single-component salts.

According to recent ORNL recommendations,[26] the following two types of salts should be studied for AHTR and LSFR primary circuits in the future:

- Salts that have been shown in the past to support the least corrosion (e.g., salts containing BeF_2 and ZrF_4 in the concentration range 25–40 mol%);

- Salts that provide the opportunity for controlling corrosion by establishing a very reducing salt environment (e.g., alkali fluoride (LiF–NaF–KF) mixtures and BeF_2-containing salts).

Alternatively, the 2400 MWt liquid-salt-cooled, flexible-conversion-ratio reactor[25] was designed, utilizing as a primary coolant the ternary chloride salt 30NaCl–20KCl–50$MgCl_2$ (in mol%) with maximum cladding temperatures under 650 °C. The selected chloride base salt has high melting points (396 °C for the reference salt vs. 98 °C for sodium). Claim is made that the materials used in the fuel, core, and vessel should be the same as those in the sodium and lead reactor designs but at temperatures required corrosion behavior for mentioned above materials in chloride salts is not clear yet (see details in **Section 5.10.6** Secondary Circuit Coolants, **Table 7**).

For applications that use molten salt outside a neutron field, additional salts may be considered. Candidate coolants can include salts deemed unsuitable as a primary coolant but judged as acceptable for use in a heat transfer loop. Familiar oxygen-containing salts (nitrates, sulfates, and carbonates) are excluded from consideration because they do not possess the necessary thermochemical stability at high temperatures (>600 °C). These salts are also incompatible with the use of carbon materials because they decompose at high temperatures to release oxygen, which rapidly reacts with the available carbon.

The screening criteria for selecting secondary salt coolants require that the elements constituting the coolant must form compounds that (1) have chemical stability at required temperatures, (2) melt at useful temperatures and are not volatile, and (3) are compatible with high-temperature alloys, graphite, and ceramics.

In addition to the fluoride salts considered (see **Table 2**), two families of salts fulfill these three basic requirements: (a) alkali fluoroborates and (b) chloride salts. For both salt systems, there are material problems, particularly at the high end of the temperature range. The chemical stability of chloride salt mixtures seems not as good as for fluorides, though exclusion of oxygen and nitrogen is important. Sulfur from ^{35}Cl and some fission products are potential precipitating species. Processing could be carried out, at some cost in external holdup. High-temperature processing has the potential benefits of being close-coupled, of reducing inventory, and of conserving ^{37}Cl.

Finally, a heat transport fluid is envisaged for the coupling of a reactor with a chemical plant, for example, for hydrogen production.[34] Typical salts considered are LiF–NaF–KF, KCl–$MgCl_2$, and KF–KBF_4. The ternary LiF–NaF–KF mixture provides superior heat transfer, KCl–$MgCl_2$ has the potential to be a very low-cost salt, and KF–KBF_4 may provide a useful barrier to isolate tritium from the hydrogen plant. Also, the ternary eutectic 9LiCl–63KCl–28$MgCl_2$ (in mol%) with melting point of 402 °C appears to be the best compromise between raw material cost, performance, and melting point.

As will be shown in the next sections, molten salts, first of all fluorides, are well suited for use at elevated temperatures as (a) fluid-fuel, (b) in-core coolant in a solid-fuel reactor, and (c) secondary coolant to transport nuclear heat at low pressures to a distant location. Materials are the greatest challenge for all high-temperature molten-salt nuclear applications. Current materials allow operation at 700–750 °C and may be extended to higher temperatures. Operating temperatures much above 800 °C will require significantly improved materials. There are strong incentives to increase the temperature to reach the full potential of the molten-salt-related systems for efficient electric and thermochemical hydrogen production. In this chapter, we review the relevant studies on materials performance in molten salts.

5.10.2.1 Chemical Compatibility of Materials with Molten-Salt Fluorides

For any high-temperature application, corrosion of the metallic container alloy is the primary concern. Unlike the more conventional oxidizing media, the products of oxidation of metals by fluoride and chloride melts tend to be completely soluble in the corroding media.[35–38] Owing to their solubility in the corroding media, passivation is precluded and the corrosion rate depends on other factors, including[39–46] oxidants, thermal gradients, salt flow rate, and galvanic coupling.

The general rule to ensure that the materials of construction are compatible (noble) with respect to the salt is that the difference in the Gibbs free energy of formation between the salt and the container material should be >80 kJ mol^{-1} K^{-1}. The corrosion strategy is the same as that used in SFR, where the materials of construction are noble relative to metallic sodium. Many additional factors will influence the corrosion of alloys in contact with salts, but it is useful to keep in mind that the fundamental thermodynamic driving force for corrosion appears to be slightly greater in chloride systems than in fluoride systems. This treatment ignores a number of important salt solution effects, especially for salt mixtures that exhibit large deviations from ideal thermodynamic behavior. Additional study in the laboratory will be needed to understand whether chloride salts are fundamentally more corrosive toward alloys than fluorides, and whether corrosion control strategies can be devised that can be used with, or favor, chloride salt systems.[34]

As mentioned above, design of a practicable MSR system demands the selection of salt constituents that are not appreciably reduced by available structural metals and alloys whose components Mo, Ni, Nb, Fe, and Cr can be in near equilibrium with the salt (see **Table 1**). Equilibrium concentrations for these components will strongly depend on the solvent system. Examination of the free energies of formation for the various alloy components shows that chromium is the most active metal components. Therefore, any oxidative attachment to these alloys should be expected to show selective attack on the chromium. Stainless steels, having more chromium than Ni-base alloys developed within MSR programs, are more susceptible to corrosion by fluoride melts, but can be considered for some applications.

Chemical reaction of the fluoride with moisture can form metal oxides that have much higher melting points and therefore appear as insoluble components at operating temperatures.[39,40] Reactions of uranium tetrafluoride with moisture result in the formation of the insoluble oxide:

$$UF_4 + 2H_2O \leftrightarrow UO_2 + 4HF \qquad [1]$$

The most direct method to avoid fuel oxide formation is through the addition of ZrF_4, which reacts in a similar way with water vapor:

$$ZrF_4 + 2H_2O \leftrightarrow ZrO_2 + 4HF \qquad [2]$$

The net reaction would be

$$ZrF_4 + UO_2 \leftrightarrow ZrO_2 + UF_4 \qquad [3]$$

Oxide films on the metal are dissolved by the following reactions:

$$2NiO + ZrF_4 \rightarrow 2NiF_2 + ZrO_2 \qquad [4]$$

$$NiO + BeF_2 \rightarrow NiF_2 + BeO \qquad [5]$$

$$2NiO + UF_4 \rightarrow NiF_2 + UO_2 \qquad [6]$$

Other corrosion reactions are possible with solvent components if they have not been purified well before utilization:

$$Cr + NiF_2 \rightarrow CrF_2 + Ni \qquad [7]$$

$$Cr + 2HF \rightarrow CrF_2 + H_2 \qquad [8]$$

These reactions will proceed essentially to completion at all temperatures within the circuit. Accordingly, such reactions can lead (if the system is poorly cleaned) to rapid initial corrosion. However, these reactions do not give a sustained corrosive attack. The impurity reactions can be minimized by maintaining low impurity concentrations in the salt and on the alloy surfaces.

Reaction of UF_4 with structural metals (M) may have an equilibrium constant which is strongly temperature dependent; hence, when the salt is forced to circulate through a temperature gradient, a possible mechanism exists for mass transfer and continued attack:

$$2UF_4 + M \leftrightarrow 2UF_3 + MF_2 \qquad [9]$$

This reaction is of significance mainly in the case of alloys containing relatively large amounts of chromium. Corrosion proceeds by the selective oxidation of Cr at the hotter loop surfaces, with reduction and deposition of chromium at the cooler loop surfaces. In some solvents (Li,Na,K,U/F, for example), the equilibrium constant for reaction [9] with Cr changes sufficiently as a function of temperature to cause the formation of dendritic chromium crystals in the cold zone.[38] For Li,Be,U/F mixtures, the temperature dependence of the mass transfer reaction is small, and the equilibrium is satisfied at reactor temperature conditions without the formation of crystalline chromium. Of course, in the case of a coolant salt with no fuel component, reaction [9] would not be a factor.

Redox processes responsible for attack by molten fluoride mixtures on the alloys result in selective oxidation of the contained chromium. This removal of chromium from the alloy occurs primarily in regions of highest temperature and results in the formation of discrete voids in the alloy.[35] These voids are not, in general, confined to the grain boundaries in the metal, but are relatively uniformly distributed throughout the alloy surface in contact with the melt. The rate of corrosion has been measured and was found to be controlled by the rate at which chromium diffuses to the surfaces undergoing attack.[41]

Graphite does not react with molten fluoride mixtures of the type to be used in the MSR concepts considered above (after carbon, borides and nitrides appear to be the most compatible nonmetallic materials). Available thermodynamic data suggest that the most likely reaction:

$$4UF_4 + C \leftrightarrow CF_4 + 4UF_3 \qquad [10]$$

should come to equilibrium at CF_4 pressures $<10^{-1}$ Pa. CF_4 concentrations over graphite–salt systems maintained for long periods at elevated temperatures have been shown to be below the limit of detection (<1 ppm) of this compound by mass spectrometry. Moreover, graphite has been used as a container material for many $NaF–ZrF_4–UF_4$, $LiF–BeF_2–UF_4$, and other salt mixtures at ORNL and the RRC-Kurchatov Institute, with no evidence of chemical instability.[47]

In an MSR, reactions such as [11] and the later [12] were prevented by careful control of the solution redox chemistry, which was accomplished by setting the UF_4/UF_3 ratio at approximately (50–60)/1:

$$UF_4 + Cr \leftrightarrow UF_3 + CrF_2 \qquad [11]$$

$$UF_3 + 2C \leftrightarrow UC_2 + 3UF_4 \qquad [12]$$

Additions of metallic Be to the fuel salt lead to reduction of the UF_4 via

$$2UF_4 + Be^0 \leftrightarrow 2UF_3 + BeF_2 \qquad [13]$$

The significance of redox control to the MOSART system with uranium-free fuel is that in some cases, where the fuel is, for example, PuF_3, the Pu(III)/Pu (IV) redox couple is too oxidizing to present a satisfactory redox-buffered system. In this case, as was proposed by ORNL, redox control could be accomplished by including an HF/H_2 mixture to the inert cover gas sparge, which will not only set the redox potential, but will also serve as the redox indicator if the exit HF/H_2 stream is analyzed relative to inlet.[48]

In principle, avoiding corrosion in an MSR or in fuel-processing units with metallic components is significantly more challenging than avoiding corrosion in clean salt coolant applications (heat transport loops, AHTR and LSFR). In an MSR, the dissolved uranium and other such species in the fuel salt result in the presence of additional corrosion mechanisms that can limit the useful service temperature of an alloy. In clean salt applications, these types of corrosion mechanisms can be reduced or eliminated by (1) using purified salts that do not contain chemical species that can transport chromium and other alloy constituents or (2) operating under chemically reducing conditions. Under chemically reducing conditions, chromium fluoride has an extremely low solubility, which limits chromium transport.

The interaction of trace amounts of oxides, air, or moisture (either in the salt or cover gas) with fluoroborates often controls alloy corrosion, but these chemical interactions are complex and are not completely understood. For the secondary coolant $NaF–NaBF_4$, corrosion is mainly determined by the selective yield of Cr from the alloy through the following reactions[45]:

$$H_2O + NaBF_4 \leftrightarrow NaBF_3OH + HF$$

$$NaBF_3OH \leftrightarrow NaBF_2O + HF$$

$$6HF + 6NaF + Cr \leftrightarrow 2Na_3CrF_6 + 3H_2 \qquad [14]$$

The hydrolysis of BF_3 in the presence of any moisture in the cover gas above the salt is rapid and generates HF which is intensely corrosive to the system, especially when it is absorbed into molten salt. Some of the actual oxygen- and hydrogen-containing species that result from hydrolysis of BF_3 in the salt have been identified. However, understanding of this chemistry is not complete,[49] and more work is needed before preparative chemistry and online purification requirements can be defined with confidence. The behavior of hydrogen- and oxygen-containing species in fluoroborates is also important because it provides a means to sequester tritium in the salt, and thus an intermediate fluoroborate loop could serve as an effective tritium barrier. The species that is likely responsible for holding tritium in the salt was identified by Maya,[50] and an engineering-scale experimental program was conducted that proved the effectiveness of sodium fluoroborate in sequestering tritium.[51]

5.10.2.2 Preparative Chemistry and Salt Purification

Molten-salt use typically begins with the acquisition of raw components that are combined to produce a mixture that has the desired properties when melted. However, most suppliers of halide salts do not provide materials that can be used directly. The major impurities that must be removed to prevent severe corrosion of the container metal are moisture/oxide contaminants. Once removed, these salts must be kept from atmospheric contamination by handling and storage in sealed containers. During the US MSR program, considerable effort was devoted to salt purification by HF/H_2 sparging of the molten salt, which is described in numerous reports.[52–55] In addition to removing moisture/oxide impurities, the purification also removes other halide contaminants such as chloride and sulfur. Sulfur is usually present in the form of sulfate and is reduced to sulfide ion, which is swept out as H_2S in the sparging operation. Methods were also developed to ensure the purity of the reagents used to purify the salts and clean the container surfaces used for corrosion testing. Another means of purification that can be performed after sparging involves simply reducing the salt with a constituent active metal such as an alkali metal, beryllium, or zirconium. While such active metals will remove oxidizing impurities such as HF, moisture, or hydroxide, they will not affect the other halide contaminants that influence sulfur removal. Therefore, it seems inevitable that the HF/H_2 sparging operation, either by itself or followed by a reducing (active metal) treatment, will be a necessity. Although a great deal of effort can be devoted to purify the molten-salt mixture in the manner described above, it is primarily useful in producing materials for research purposes, without the possibility of interference from extraneous impurities.

Removal of oxygen-containing impurities from chloride and fluoroborate salts is considerably more difficult because the fluoride ion more readily displaces oxygen from most compounds than does the chloride ion and because borate and hydroxyborate impurities are difficult to remove by fluorination with HF.

Nearly all of the chloride salts prepared for corrosion studies have had relatively high levels of oxygen-containing impurities. The typical salt preparation for these studies involved treatment of reagent chlorides by drying the solid salt under vacuum, followed by prolonged treatment with dry HCl gas, and finishing with an inert gas purge of HCl from the salt. This treatment is not effective in removing the last portion of bound oxygen from the salt. Depending on the salt composition, oxygen contents of up to a few percent (in wt%) may remain. A more effective method for removing oxygen is needed to investigate the basic corrosion mechanism in pure chloride salts; otherwise, the effects of oxygen-containing species will dominate the apparent corrosion response. The use of carbochlorination has been recommended[56] for the removal of oxygen and it has been claimed that salts with very low oxygen content ($\sim$3 ppm) can be produced by this method.[57]

A similar type of purification improvement is needed for fluoroborates. Previous treatments with HF and BF_3 (to avoid loss of BF_3 from the melt) were not as effective as desired. There is also a need for accurate analytical methods for the determination of oxygen in melts and, in certain cases, it is necessary to identify the oxygen-containing species (oxide type, hydroxyl, etc).

5.10.3 Developments in Materials for Different Reactor Systems

5.10.3.1 Molten-Salt Reactor

When considering an MSR, the materials required fall into three main categories: (1) metallic components for primary and secondary circuits, (2) graphite in the core, and (3) materials for molten-salt fuel reprocessing systems.

The metallic material used in constructing the primary circuit of an MSR will operate at temperatures up to 700–750 °C. The outside of the primary circuit will be exposed to nitrogen containing sufficient air from inleakage to make it oxidizing to the metal. No metallic structural members will be located in the highest flux. The inside of the circuit, depending on design, will be exposed to salt-containing fission products and will receive maximum fast and thermal fluencies of about $1–2 \times 10^{20}$ and $5–8 \times 10^{21}$ neutrons cm^{-2}, respectively. The operating lifetime of a reactor will be in the range of 30–50 years, with an 80% load factor. Thus, the metal must have moderate oxidation resistance, must resist corrosion by the salt, and must not be subject to severe embrittlement by neutrons.[49] The material must be fabricable into many products (plate, piping, tubing, and forgings) and capable of being formed and welded both under well-controlled shop conditions and in the field. The primary circuit involves numerous structural shapes ranging from a few centimeters thick to tubing having wall thicknesses <1 mm. These shapes must be fabricated and joined, primarily by welding, into an integral engineering structure. Thus, the activities required for development of material for the primary circuits will suffice for secondary circuits if supplemented by information on the compatibility of the material with the coolant salt.

Graphite is the principal material other than salt in the core of the reference breeder reactor design with a thermal spectrum and thorium fuel cycle.[16,17] In nonmoderated MSR concepts (e.g., MOSART[1] and MSFR[4]), graphite is used only as a reflector.

The graphite core and reflector structures will operate in a fuel salt environment over a range of temperatures from 500 up to 800 °C. In any MSR design, graphite is, of course, subject to radiation damage. There are two overriding requirements in the graphite in MSRs, namely, that both molten salt and xenon be excluded from open pore volume. Any significant penetration of the graphite by the fuel-bearing salt would generate a local spot, leading to enhanced radiation damage to the graphite and perhaps local boiling of the salt. This requires that the graphite be free of gross structural defects and that the pore structure be largely confined to diameters $<10^{-6}$ m.[49] ^{135}Xe will diffuse into graphite and affect the neutron balance. This requires graphites of very low permeability, for example, $10^{-8}\ cm^2\ s^{-1}$. The requirements of purity and impermeability to salt are easily met by high-quality, fine-grained graphite, and the main problems arise from the requirement of stability against radiation-induced distortion.[58]

Material selection for molten-salt fuel reprocessing systems depends, of course, upon the nature of the chosen process and the design of the equipment to implement the process. For MSRs,[58] the key operations in fuel reprocessing are (1) removal of uranium from the fuel stream for immediate return to the reactor, (2) removal of ^{233}Pa and fission product zirconium from the fuel for isolation and decay of ^{233}Pa outside the neutron flux, and (3) removal of rare-earth, alkali-metal, and alkaline-earth fission products from the fuel solvent before its return, along with the actinides, to the reactor. Such a processing plant will present a variety of corrosive environments. The most severe ones are (a) the presence of molten salt along with gaseous mixtures of F_2 and UF_6 at 500 °C and that with absorbed UF_6, so the average valence of uranium is near 4.5 ($UF_{4.5}$) at temperatures near 550 °C and (b) the presence of molten salts (either molten fluorides or molten LiCl) and molten alloys containing bismuth, lithium, thorium, and other metals at temperatures near 650 °C as well as HF–H_2 mixtures and molten fluorides, along with bismuth in some cases, at 550–650 °C. High radiation and contamination levels will require that the processing plant be contained and have strict environmental control. If the components are constructed of reactive materials, such as molybdenum, tantalum, or graphite, the environment must be an inert gas or a vacuum to prevent deterioration of the structural material. Obviously, materials capable of long-term service under these conditions must be provided.

The main developments necessary to do this within the above-mentioned categories are described below.

5.10.3.1.1 Metallic materials for primary and secondary circuits

An extremely large body of literature exists on the corrosion of metal alloys by molten fluorides. Much of this work was done at ORNL and involved either thermal convection or forced convection flow loops. To select the alloy best suited to this application, an extensive program of corrosion tests was carried out on the available commercial nickel-base alloys and austenitic stainless steels.[26,34–38]

5.10.3.1.1.1 Development status of nickel-base alloys in ORNL

These tests were performed in a temperature gradient system with various fluoride media and different temperatures (maximum temperature and temperature gradient). Chromium, which is added to most alloys for high-temperature oxidation resistance, is quite soluble in molten fluoride salts. Metallurgical examination of the surveillance specimens showed corrosion to be associated with outward diffusion of Cr through the alloy. It was concluded that the chromium content should be maintained as low as reasonably possible to keep appropriate air oxidation properties. Corrosion rate is marked by initial rapid attack associated with dissolution of Cr and is largely driven by impurities in the salt.[26,34–38] This is followed by a period of slower, linear corrosion rate behavior, which is controlled by a mass transfer mechanism dictated by thermal gradients and flow conditions. Minor impurities in the salt can enhance corrosion by several orders of magnitude and must be kept to a minimum. Dissolution can be mitigated by a chemical control of the redox in salts, for example, by small additions of elements such as Be. Corrosion increased dramatically as the temperature was increased and is coupled to plate-out in the relatively cooler regions of the system, particularly in situations where high flow is involved.

The nuclear power aircraft application for which MSRs were originally developed required that the fuel salt operate at around 850 °C. Inconel 600, out of which the Na,Zr,U/F ARE test reactor was built, was not strong enough and corroded too rapidly at the design temperature for long-term use.[12–14] The existing alloys were screened for corrosion resistance at this temperature and only two were found to be satisfactory: Hastelloy B (Ni–28% Mo–5% Fe) and

Hastelloy W (Ni–25% Mo–5% Cr–5% Fe). However, both aged at service temperature and became quite brittle due to formation of Ni–Mo intermetallic compounds.[38] On the other hand, Hastelloy B, in which chromium is replaced with molybdenum, shows excellent compatibility with fluoride salts at temperatures in excess of 1000 °C. Unfortunately, Hastelloy B cannot be used as a structural material in high-temperature systems because of its age-hardening characteristics, poor fabrication ability, and oxidation resistance. Tests performed at 815 °C especially showed Ni-base alloys to be superior to Fe-base alloys. This led to the development of a tailored Ni-base alloy, called INOR-8 or Hastelloy N (see **Table 3**), with a composition of Ni–16% Mo–7% Cr–5% Fe–0.05% C.[35] The alloy contained 16% molybdenum for strengthening and chromium sufficient to impart moderate oxidation resistance in air, but not enough to lead to high corrosion rates in salt. Hastelloy N has excellent corrosion resistance to molten fluoride salts at temperatures considerably above those expected in MSR service; further (see **Table 4**), the resultant maximum corrosion rate of Hastelloy N measured in extensive Li,Be,Th,U/F loop testing at reactor operating temperatures was below 5 μm $year^{-1}$.[42–46] Higher redox potential set in the system Li,Be,Th,U/F made the salt more oxidizing. At ORNL, the dependence of corrosion versus flow rate was tested in the range of velocities from 1 to 6 m s^{-1}. It was reported that the influence of the flow rate was significant only during the first 1000–3000 h. Later, the corrosion rates, as well as their difference, decreased.[43]

The mechanical properties of Hastelloy N at operating temperatures are superior to those of many stainless steels and are virtually unaffected by long-time exposure to salts. The material is structurally stable in the operating temperature range, and the oxidation rate is <2 mils in 100 000 h. No difficulty is encountered in fabricating standard shapes when the commercial practices established for nickel-base alloys are used. Tubing, plates, bars, forgings, and castings of Hastelloy N have been made successfully by several major metal manufacturing companies, and some of these companies are prepared to supply it on a commercial basis. Welding procedures have been established, and a good history of reliability of welds exists. The material has been found to be easily weldable with a rod of the same composition. Inconel is, of course, an alternate choice for the primary circuit structural material, and much information is available on its compatibility with molten salts and sodium. Although probably adequate, Inconel does not have the degree of flexibility that Hastelloy N has in corrosion resistance to different salt systems, and its lower strength at reactor operating temperatures would require heavier structural components.

Hastelloy N alloy was the sole structural material used in the Li,Be,Zr,U/F MSRE and contributed

Table 3 Chemical composition of the nickel–molybdenum alloys (mass %)

Element	*Hastelloy N (INOR-8)*	*Ti-modified Hastelloy N 1972*[58]	*Nb-modified Hastelloy 1976*[58]	*HN80M-VI*	*HN80MTY (EK-50)*	*MONICR*
Ni	Base	Base	Base	Base	Base	Base
Cr	7.52	6–8	6–8	7.61	6.81	6.85
Mo	16.28	11–13	11–13	12.2	13.2	15.8
Ti	0.26	2	–	0.001	0.93	0.026
Fe	3.97	0.1	0.1	0.28	0.15	2.27
Mn	0.52	0.15–0.25	0.15–0.25	0.22	0.013	0.037
Nb	–	0–2	1–2	1.48	0.01	<0.01
Si	0.5	0.1	0.1	0.040	0.040	0.13
Al	0.26	–	–	0.038	1.12	0.02
W	0.06	–	–	0.21	0.072	0.16
Cu	0.02	–	–	0.12	0.020	0.016
Co	0.07	–	–	0.003	0.003	0.03
Ce	–	–	–	0.003	0.003	<0.003
Zr	–	–	–	–	–	0.075
B	<0.01	0.001	0.001	0.008	0.003	<0.003
S	0.004	0.01	0.01	0.002	0.001	0.003
P	0.007	0.01	0.01	0.002	0.002	0.003
C	0.05	0.05	0.05	0.02	0.025	0.014

– The elements were neither added to the melt nor determined.

Table 4 Summary of ORNL loop corrosion tests for fuel fluoride salts

Test loop	*Structural material*	*Molten salt (mol%)*	*Fluid test conditions*				*Specim. temperature (°C)*	*Corrosion rate (μm year^{-1})*
			Circulation mode	*T_{max} (°C)*	*T_{max} (°C)*	*Exposure (h)*		
NCL-1255	Hastelloy N + 2% Nb	70LiF–23BeF_2–5ZrF_4–1UF_4–1ThF_4	Natural convection	704	90	80 439	–	–
NCL-16	Hastelloy N	66.5LiF–34BeF_2–0.5UF_4	Natural convection $V = 2.5\ cm\ s^{-1}$	704	170	28 000	660	1.0
	Hastelloy N						675	0.5
	mod. Ti $\leq$ 0.5						700	0.9
MSRE	Hastelloy N	65LiF–29.1BeF_2–5.0–ZrF_4–0.9UF_4	Fuel circuit	654	22	21 800	654	8.0
		66LiF–34BeF_2	Coolant circuit	580	35	26 100	580	no
NCL-15A	Hastelloy N	73LiF–2BeF_2–5ThF_4	Natural convection	677	55	35 400	677	1.5
NCL-18	Hastelloy N	68LiF–20BeF–11.7ThF–0.3UF_4	Natural convection	704	170	11 600	704	1.2
NCL-21A	Hastelloy N	71.7LiF–16BeF_2–12ThF_4–0.3UF_4	Natural convection	704	138	10 009	704	3.5
	Hastelloy N, mod. 1% Nb	$U^{4+}/U^{3+} \approx 104$	$V = 1\ cm\ s^{-1}$			1004	704	3.7
NCL-23	Inconel 601	71.7LiF–16BeF_2–12ThF_4–0.3UF_4 $U^{4+}/U^{3+} \approx 40$	Natural convection $V = 1\ cm\ s^{-1}$	704	138	721	704	$\geq$34
NCL-24	Hastelloy N, mod. 3.4% Nb	68LiF–20BeF–11.7ThF–0.3UF_4	Natural convection	704	138	1500	704	2.5
FCL-2b	Hastelloy N	71.7LiF–16BeF_2—12ThF_4–0.3UF_4	Forced convection	704	138	4309	704	2.6
	Hastelloy N mod. 1% Nb	$U^{4+}/U^{3+} \approx 100$	$V = 2.5–5\ m\ s^{-1}$			2242	704	0.4

Source: Koger, J. W. Alloy compatibility with LiF–BeF_2 salts containing ThF_4 and UF_4, ORNL-TM-4286; ORNL: Oak Ridge, TN, 1972; Keiser, J. R.; *et al.* Salt corrosion studies, ORNL-5078; ORNL: Oak Ridge, TN, 1975; pp 91–97; Keiser, J. R. Compatibility studies of potential molten-salt breeder reactor materials in molten fluoride salts, ORNL-TM-5783; ORNL: Oak Ridge, TN, 1977.

significantly to the success of the experiment.[15,16] Less severe corrosion attack (<20 μm year^{-1}) was seen for the Hastelloy N in contact with the MSRE fuel salt at temperatures up to 704 °C for 3 years (26 000 h). The most striking observation is the almost complete absence of corrosion for Hastelloy N during the 3-year exposure to the MSRE coolant Li,Be/F salt (see **Table 4**).

Two main problems of Hastelloy N requiring further study were observed during the construction and operation of the MSRE. The first was that the Hastelloy N used for the MSRE was subject to a kind of 'radiation hardening,' due to accumulation of helium at grain boundaries.[59,60] Later, it was found that modified alloys with fine carbide precipitates within the grains would hold the helium and avoid this migration to the grain boundaries. Nevertheless, it is still desirable to design well-blanketed reactors in which the exposure of the reactor vessel wall to fast neutron radiation is limited. The second problem was the discovery of tiny cracks on the inside surface of the Hastelloy N piping for the MSRE. It was found that these cracks were caused by the fission product tellurium.[61,62] Later work showed that tellurium attack could be controlled by keeping the fuel under reducing conditions.[63–65] This is done by adjustment of the chemistry so that about 2% of the uranium is in the form of UF_3, as opposed to UF_4. This can be controlled rather easily now that good analytical methods have been developed. If the UF_3 to UF_4 ratio becomes too low, it can be raised by the addition of some beryllium metal, which, as it dissolves, will rob some of the fluoride ions from the uranium.

When the ORNL studies were terminated in early 1973, considerable progress had been made in finding solutions to both problems.[58] Since the two problems were discovered a few years apart, the research on them appears to have proceeded independently. However, the work must be brought together for the production of a single material resistant to both problems. It was found that the carbide precipitate that normally occurs in Hastelloy N could be modified to obtain resistance to embrittlement by helium. The presence of 16% molybdenum and 0.5% silicon led to the formation of coarse carbide that was of little benefit. Reduction of the molybdenum concentration to 12% and the silicon content to 0.1% and the addition of a reactive carbide former such as titanium led to the formation of a fine carbide precipitate and an alloy with good resistance to embrittlement by helium. The desired level of titanium was about 2%, and the phenomenon was confirmed by numerous small laboratories and commercial melts by 1972.

Because the intergranular embrittlement of Hastelloy N by tellurium was noted in 1970, ORNL's understanding of the phenomenon was not very advanced at the conclusion of the program in 1973. Numerous parts of the MSRE were examined, and all surfaces exposed to fuel salt formed shallow intergranular cracks (IGC) when strained. Some laboratory experiments had been performed in which Hastelloy N specimens were exposed to low partial pressures of tellurium metal vapor and, when strained, formed IGC very similar to those noted in parts from the MSRE. Several findings indicated that tellurium was the likely cause of the intergranular embrittlement, and the selective diffusion of tellurium along the grain boundaries of Hastelloy N was demonstrated experimentally. One in-reactor fuel capsule was operated in which the grain boundaries of Hastelloy N were embrittled and those of Inconel 601 (Ni, 22% Cr, 12% Fe) were not. These findings were in agreement with laboratory experiments in which these same metals were exposed to low partial pressures of tellurium metal vapor. Thus, at the close of the program in early 1973, tellurium had been identified as the likely cause of intergranular embrittlement, and several laboratory and in-reactor methods were devised for studying the phenomenon. Experimental results had been obtained that showed variations in sensitivity to embrittlement of various metals and offered encouragement that a structural material could be found that resisted embrittlement by tellurium.

The alloy composition favored at the close of the ORNL program in 1973 is given in **Table 3** with the composition of standard Hastelloy N. The reasoning at that time was that the 2% titanium addition would impart good resistance to irradiation embrittlement and the 0–2% niobium addition would impart good resistance to intergranular tellurium embrittlement. Neither of these chemical additions was expected to cause problems with respect to fabrication and welding.

When the ORNL program was restarted in 1974, top priority was given to the tellurium-embrittlement problem.[63–66] A small piece of Hastelloy N foil from the MSRE had been preserved for further study. Tellurium was found in abundance, and no other fission product was present in detectable quantities. This showed even more positively that tellurium was responsible for the embrittlement.

Considerable effort was spent in seeking better methods of exposing test specimens to tellurium.

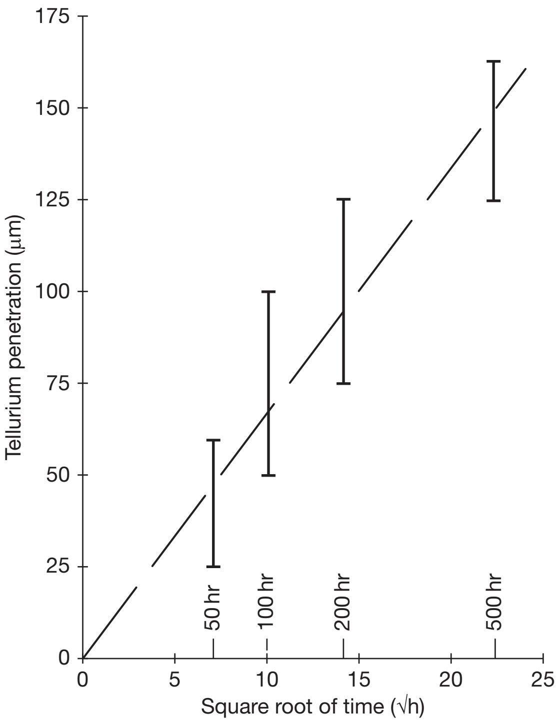

Figure 1 Tellurium penetration versus time for Hastelloy N exposed at 700 °C to LiF–BeF_2–ThF_4 (72–16–12 mol%) containing Cr_3Te_4. Data obtained by Atomic Energy Station (AES). Reproduced from Keiser, J. R. Status of tellurium–Hastelloy N studies in molten fluoride salts, ORNL-TM-6002; ORNL: Oak Ridge, TN, 1977.

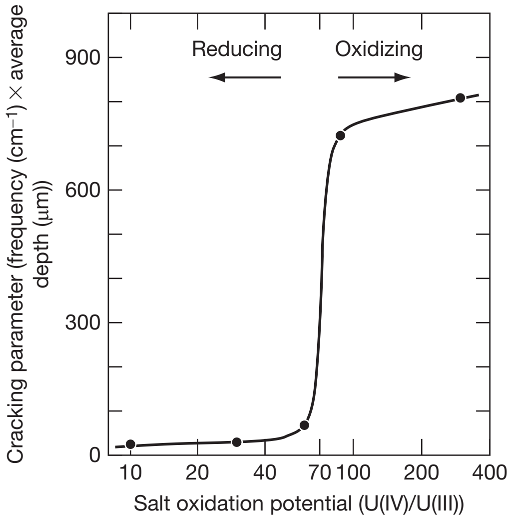

Figure 2 Cracking behavior of Hastelloy N exposed for 260 h at 700 °C to molten-salt breeder reactor fuel salt containing Cr_3Te_4 and Cr_5Te_6. Reproduced from Mc Coy, H. E.; *et al.* Status of materials development for molten-salt reactors, ORNL-TM-5920; ORNL: Oak Ridge, TN, 1978.

The most representative experimental system developed for exposing metal specimens to tellurium involved suspending the specimens in a stirred vessel of salt with granules of Cr_3Te_4 and Cr_5Te_6 lying at the bottom of the salt. Tellurium, at a very low partial pressure, was in equilibrium with the Cr_3Te_4 and Cr_5Te_6, and exposure of Hastelloy N specimens to this mixture resulted in crack severities similar to those noted in samples from the MSRE (see Figure 1).

As a result of these studies,[65,66] it was found that Hastelloy N exposed in salt-containing metal tellurides, such as Li_xTe and Cr_yTe_x, undergoes grain boundary embrittlement similar to that observed in the MSRE. The embrittlement is a function of the chemical activity of tellurium associated with the telluride. Controlling the oxidation potential of the salt coupled with the presence of chromium ions in the salt appears to be an effective means of limiting tellurium embrittlement of Hastelloy N. The degree of embrittlement can be reduced by alloying additions to the Hastelloy N. The addition of 1–2 mass % Nb significantly reduces embrittlement, but small additions of titanium or additions of up to 15 at.% Cr do not affect embrittlement. It was found that if the U(IV)/U(III) ratio in fuel salt is kept below about 60, embrittlement is essentially prevented when $CrTe_{1.266}$ is used as the source of tellurium (see Figure 2). However, further studies are needed to assess the effects of longer exposure times and measure the interaction parameters for chromium and tellurium under varying salt oxidation potentials.

Studies of irradiation embrittlement and intergranular tellurium embrittlement have progressed to the point where suitable options are available. Postirradiation creep properties were acceptable for Hastelloy N modified with 2% Ti, 1–4% Nb, or about 1% each of Nb and Ti. The 2%-Ti-modified alloy was made into a number of products, and some problems with cracking during annealing were encountered. The other alloys were only fabricated into 1/2-in.-thick plates and 1/4-in.-diameter rods, and no problems were encountered. All alloys had excellent weldability. There are no obvious reasons why all of these alloys cannot be fabricated after development of suitable scale-up techniques.

The resistance of all of these alloys to irradiation embrittlement depends upon the formation of a fine dispersion of MC-type carbide particles. These particles act as sites for trapping He and prevent it from reaching the grain boundaries where it is embrittling.

These alloys would be annealed after fabrication into basic structural shapes and the fine carbides would precipitate during service in the temperature range from 500 to 650 °C. If the service temperature exceeds this range significantly, the carbides begin to coarsen, and the resistance to irradiation embrittlement diminishes. Although some heated specimens of the 2%-Ti-modified alloys and 3–4%-Nb-modified alloys had acceptable properties after irradiation at 760 °C, it is very questionable whether these alloys can realistically be viewed for service temperatures above 650 °C.

One very important development related to intergranular embrittlement by tellurium was a number of experimental methods for exposing test metals to tellurium under fairly realistic conditions. The use of metal tellurides, which produce low partial pressures of tellurium at 700 °C, as sources of tellurium provided experimental ease and flexibility. The in-reactor fuel capsules also proved to be very effective experiments for exposing metals to tellurium and other fission products. The observation that the severity of cracking in standard Hastelloy N was influenced by the oxidation state of the salts adds the further experimental complexity that the oxidation state must be known and controllable in all experiments involving tellurium.

It is unfortunate that Ti-modified alloys were developed so far because of their good resistance to irradiation embrittlement before it was learned that the titanium addition, even in conjunction with Nb, resulted in alloys that were embrittled by Te as badly as standard Hastelloy N. However, this situation was due to the time spread of almost 6 years between discoveries of the two problems and could not be prevented. The addition of 1–2% Nb to Hastelloy N resulted in alloys with improved resistance to IGC by tellurium, but that did not totally resist cracking. Samples of these alloys were exposed to Te-containing environments for more than 6500 h at 700 °C with very favorable results (see **Figure 3**). However, cyclic tests where crack propagation is measured in the presence of Te will be required to clarify whether the Nb-modified alloys have adequate resistance to Te. The mechanism of improved cracking resistance due to the presence of Nb in the alloy is not known, but it is hypothesized that Nb forms surface reaction layers with the Te in preference to its diffusion into the metal along grain boundaries.

Screening experiments with various alloys elucidated some other possibilities. Nickel-base alloys containing 23% Cr (Inconel 601) resisted cracking,

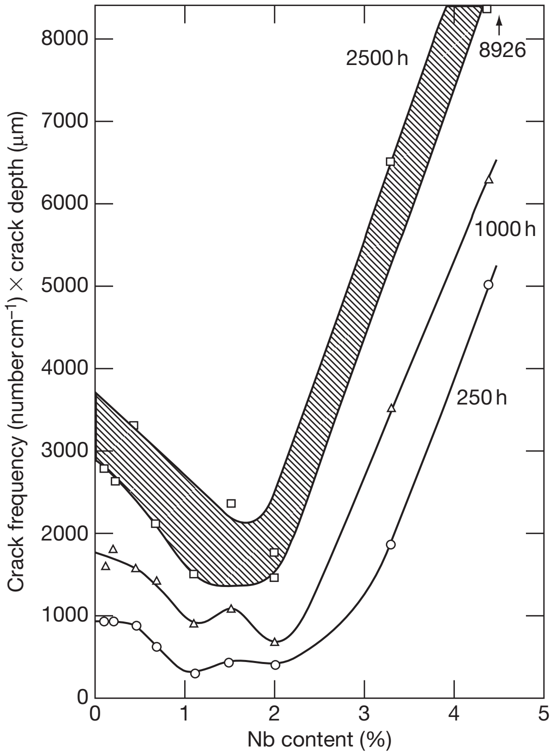

Figure 3 Variations of severity of cracking with Nb content. Samples were exposed for the indicated times to salt-containing Cr_3Te_4 and Cr_5Te_6 at 700 °C. Reproduced from Mc Coy, H. E.; *et al.* Status of materials development for molten-salt reactors, ORNL-TM-5920; ORNL: Oak Ridge, TN, 1978.

whereas alloys containing 15% Cr (Inconel 600, Hastelloy S, and Cr-modified Hastelloy N) cracked as badly as standard Hastelloy N. However, it is questionable whether the corrosion rate of alloys containing 23% Cr would be acceptable in salt. Type 304 stainless steel and several other iron-base alloys were observed to resist intergranular embrittlement, but these alloys also have questionable corrosion resistance in fuel salts. Alloys containing appreciable quantities of chromium are attacked by molten salts, mainly by the removal of chromium from hot-leg sections through reaction with UF_4, if present, and with other oxidizing impurities in the salt. The removal of chromium is accompanied by the formation of subsurface voids in the metal. The depth of void formation depends strongly on the operating temperatures of the system and on the composition of the salt mixture. If 300 series stainless steels are exposed to uranium-fueled salt under the same closed system conditions, the corrosion is manifested in surface voids of decreased Cr content to a depth of

60–70 μm at 600–650 °C. Data on corrosion rates obtained in experiments with molten Li,Be,Th,U/F mixtures for 304SS and 316SS at ORNL[42] as well as later at the RRC-Kurchatov Institute[19] for the Russian-made austenitic steels 12H18N10T (Fe–18% Cr–10% Ni–1% Ti–0.12% C) and AP-164 (Fe–15% Cr–24% Ni–1.5% Ti–4% W–0.08% C) agree well with each other.

It is possible that a salt can be made adequately reducing to allow iron-base alloys to be used. This possibility must be pursued experimentally, because thermodynamic and kinetic data are not available to allow analytical determination.

The discoveries that cracking severity was influenced by the oxidation state of the salt and that the salt could be made sufficiently reducing to prevent cracking in standard Hastelloy N opened many doors. Thus, alloys containing Ti could be used to take advantage of their excellent resistance to irradiation damage if they were protected from cracking by Te. Even standard Hastelloy N could be used in part of the system where the neutron flux was very low.

The research toward finding a material for constructing an MSR that has adequate resistance to irradiation embrittlement and IGC by tellurium has progressed. ORNL findings suggest very strongly that an MSR could be constructed of 1–2%-Nb-modified Hastelloy N and operated very satisfactorily at 650 °C.

5.10.3.1.1.2 Progress on Ni–Mo alloy development at RRC-Kurchatov Institute

In Russia, materials testing for the Th–U MSR were started at the RRC-Kurchatov Institute in 1976.[19,20,47] It was substantiated by data accumulated in the ORNL MSR program on nickel-base alloys for UF_4-containing salts. The Ni-base alloy HN80MT was chosen as a base. Its composition (in wt%) is Ni–6.9% Cr–0.02% C–1.6% Ti–12.2% Mo–2.6% Nb. The development and optimization of the HN80MT alloy was envisaged to be performed in two directions: improvement of alloy resistance to selective chromium corrosion and increase in alloy resistance to tellurium intergranular corrosion and cracking.

About 70 differently alloyed specimens of HN80MT were tested. Among alloying elements were W, Nb, Re, V, Al, Mn, and Cu. The main finding was that alloying by aluminum with a decrease of titanium to 0.5% revealed significant improvement in both the corrosion and mechanical properties of the alloy. Chromium corrosion and intergranular corrosion reached the minimum value at an aluminum content in the alloy of ~2.5%. Irradiation effect on corrosion activity of fuels was also studied. It was shown that there was no radiation-induced corrosion at least up to a power density of 10 W/cm^3 in a molten LiF–BeF_2–ThF_4–UF_4 mixture.

A subsequent radiation study of 13 alloy modifications was conducted. Specimens (in nitrogen atmosphere) were exposed to the reactor neutron field up to the fluency of 3×10^{20} neutrons cm^{-2}. Mechanical properties of alloys were studied at temperatures of 20, 400, and 650 °C for nonirradiated and irradiated specimens. The best postirradiation properties were shown for alloys modified by Ti, Al, and V.

Lastly, corrosion under the stressed condition was studied. It is known that tensile strain promotes an opening of intergranular boundaries and thus boosts intergranular corrosion and creates the prerequisites for IGC. The studies did not reveal any dependence of intergranular corrosion on the stress up to the value 240 MPa, that is, 0.8 of a tensile yield of the material and 5 times higher than typical stresses in Li,Be,Th,U/F MSR designs.

The results of the combined investigation of mechanical, corrosion, and radiation properties of various alloys of HN80MT permitted the RRC-Kurchatov Institute to suggest the Ti- and Al-modified alloy as an optimum container material for the MSR design. This alloy, named HN80MTY (or EK-50), has the composition given in **Table 3**.

In the thermal convection loop operated with the molten Li,Be,Th,U/F salt system, the HN80MTY alloy specimens have shown a maximum corrosion rate of 6 μm year^{-1} (see **Table 5**) as for the HN80MT alloy it was two times lower.[20,67] The corrosion was accompanied by selective leaching of chromium into the molten salt, which was evidenced by the 10-fold increase in its concentration for 500 h of exposure. Similar oxidizing conditions, characterized by the same content of Fe and Ni impurities in the salt, existed in testing a standard Hastelloy N alloy on the NCL-21A loop (see **Table 4**) operated with a molten Li,Be,Th,U/F salt system at ORNL.[46] For the NCL-21A loop, the uniform corrosion rate of Hastelloy N specimens was about 5 μm year^{-1}. However, in the NCL-21A loop, the maximum temperature was somewhat lower (704 °C) than in the RRC-Kurchatov Institute experiments (750 °C), and in addition, fission products, including Te, were not added into the circuit.

A comparison with corrosion data obtained at ORNL[43,46] indicates that the HN80MT and

Table 5 Summary of Russian loop corrosion tests for fluoride salts

Loop	*Salt (mol%)*	*Specimen material*	*T_{max} (°C)*	*ΔT (°C)*	*Duration (h)*	*Corrosion rate (μm year^{-1})*
Solaris	46.5LiF–11.5NaF–42KF	12H18N10T	620	20	3500	50
		HN80MT				22
KI C1	$92NaBF_4$–8NaF	12H18H10T	630	100	1000	250
KI C2		AP-164	630	100	1000	50
KI C3		HN80MT	630	100	1000	12
KI F1	71.7LiF–$16BeF_2$–	HN80MT	750	70	1000	3.0
KI F2	$12ThF_4$–$0.3UF_4$ + Te	HN80MTY	750	70	1000	6.0
KI M1	66LiF–$34BeF_2$ + UF_4	12H18N10T	630	100	500	20
KURS-2	66LiF–$34BeF_2$ + UF_4	12H18N10T	750	250	750	25
VNIITF	LiF–NaF–BeF_2 + PuF_3	HN80MT	700	100	1600	5
		HN80MTY				5
		MONICR				19
KI T1	LiF–NaF–BeF_2 + Cr_3Te_4	HN80MT	700	10	400	3
		HN80MTY				3
		MONICR				15

AP-164 alloy with a composition of Fe–22–25% Ni–14–16% Cr–4–5% W–0.5–1% Mn–1.4–1.8Ti–0.6% Si–0.08% C–0.035% P and 12H18N10T stainless steel with a composition of Fe–11–13% Ni–17–19% Cr–2% Mn–0.6–0.8% Ti–0.8% Si–0.12% C–0.035% P.
Source: Novikov, V. M.; Ignatiev, V. V.; Fedulov, V. I.; Cherednikov, V. N. *Molten Salt Reactors: Perspectives and Problems*; Energoatomizdat: Moscow, USSR, 1990; Ignatiev, V. V.; Novikov, V. M.; Surenkov, A. I.; Fedulov, V. I. The state of the problem on materials as applied to molten-salt reactor: Problems and ways of solution, Preprint IAE-5678/11; Institute of Atomic Energy: Moscow, USSR, 1993.

HN80MTY resistance is higher than that of the standard Hastelloy N. This conclusion is confirmed by the microphotographs of HN80MT and HN80MTY alloy specimens after corrosion tests. Physical metallurgy studies were done on longitudinal metallographic sections of specimens subjected to tensile tests (see **Figures 4** and **5**).

Under static conditions at $T = 600\,°C$, there is only a slight tendency of HN80MT to IGC, and corrosion defects are observed along grain boundaries at a depth of 20–30 μm. With an increase of temperature to 750 °C, the defect depth increases to 60 μm. Transition to loop tests at $T = 750\,°C$ show even more expressed IGC (see **Figure 4**). Massive defects in the material along the grain boundaries at full depth and further cracking over boundaries of the following grains were found. The defect area reached 130 μm. The alloy resistance to IGC was estimated from a parameter K, which is equal to the product of the number of cracks on a 1-cm length of a longitudinal section of specimens subjected to tensile strain multiplied by an average crack depth in micrometers. The estimated value for the parameter K in these conditions (ampoule isothermal tests at $T = 750\,°C$) amounts to 1300 pc μm cm^{-1}. For the HN80MT alloy, this value is more than 5 times lower than that of a standard Hastelloy N alloy subjected to similar testing conditions.[66]

Therefore, the maximum operating temperature for HN80MT alloy in a reactor should be reduced at least to 700 °C, and rigorous control of oxidation–reduction potential of the fuel salt is necessary. A completely different picture was observed in testing HN80MTY alloy specimens. No IGC traces were found, both in static tests under stress conditions (at 650–800 °C up to 245 MPa) and in thermal convection loops up to $T = 750\,°C$.[20,67] The thermal convection tests show that corrosion proceeds uniformly along the entire grain volume, giving rise to a small porous layer near the material surface in contact with the fuel salt at the depth of 15–30 μm (see **Figure 5**). Thus, choosing effective alloying additions can solve the problem of IGC for nickel alloys in fuel salts containing fission products. The corrosion and other characteristics of the developed HN80MTY alloy makes it possible to consider it as a promising structural material for Th–U MSRs with a maximum working temperature of 750–800 °C.[20]

The weldability of the alloy, however, needs improvement. To suppress crack formation during welding, the metal penetration regime was set up and maximum heat removal from the welded joint was ensured. These measures made it possible to increase significantly the characteristics of the welded joints. The manufacturing of a heat exchanger

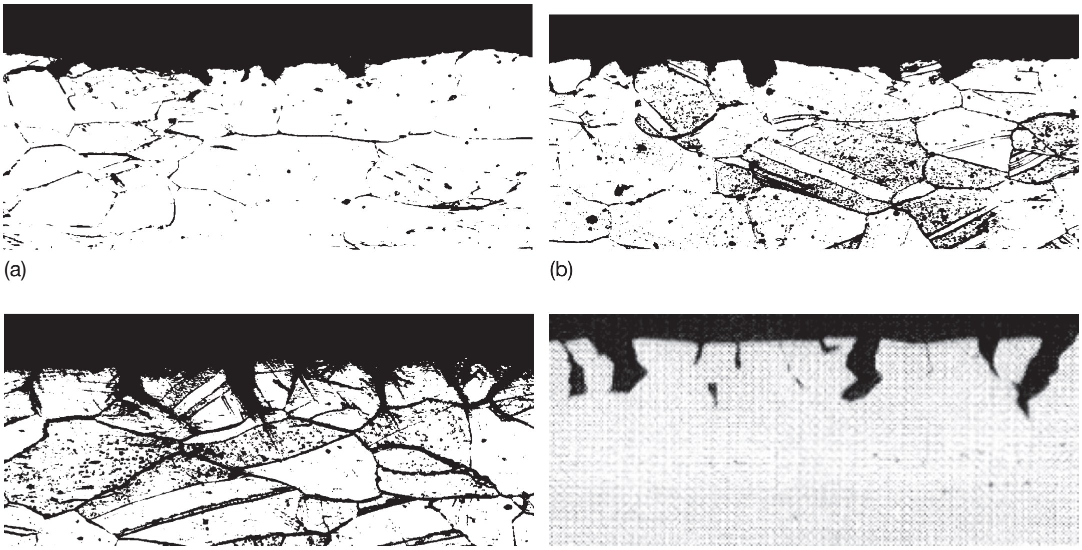

(a) (b) (c) (d)

Figure 4 Microphotographs of the Ni–Mo alloy specimen surface layer (enlargement ×100) after 500 h exposure to tellurium containing melt 71.7LiF–16BeF_2–12ThF_4–0.3UF_4. (a) HN80MT isothermal tests, $T_{exposure}$ = 600 °C; (b) HN80MT isothermal tests, $T_{exposure}$ = 750 °C; (c) HN80MT nonisothermal tests in loop, $T_{exposure}$ = 750 °C; (d) standard Hastelloy N isothermal tests, $T_{exposure}$ = 700 °C. Reproduced from Ignatiev, V. V.; Novikov, V. M.; Surenkov, A. I.; Fedulov, V. I. The state of the problem on materials as applied to molten-salt reactor: Problems and ways of solution, Preprint IAE-5678/11; Institute of Atomic Energy: Moscow, USSR, 1993.

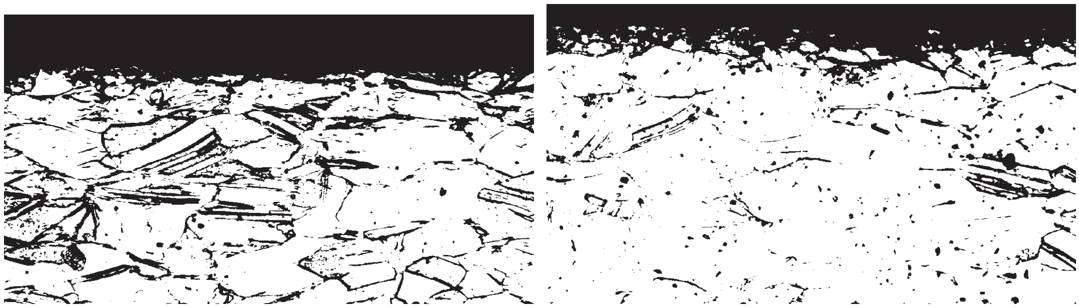

(a) (b)

Figure 5 Microphotographs of HN80MTY alloy specimens surface layer (enlargement ×100) after 500 h exposure to the tellurium containing melt 71.7LiF–16BeF_2–12ThF_4–0.3UF_4. (a) Isothermal tests, $T_{exposure}$ = 750 °C and (b) nonisothermal tests in loop, $T_{exposure}$ = 750 °C. Reproduced from Ignatiev, V. V.; Novikov, V. M.; Surenkov, A. I.; Fedulov, V. I. The state of the problem on materials as applied to molten-salt reactor: Problems and ways of solution, Preprint IAE-5678/11; Institute of Atomic Energy: Moscow, USSR, 1993.

confirmed once more that the HN80MTY alloy is technologically effective both in hot and cold process stages.[19]

In a recent study, the central focus of the corrosion studies was the compatibility of Ni-base alloys with a molten Li,Na,Be/F salt system as applied to the primary circuit of MOSART fuelled with different compositions of actinide trifluorides from LWR spent fuel without U–Th support.[68–70] Prior ORNL examinations[71] of Inconel in natural convection loops, which circulated molten 24LiF–53NaF–23BeF_2 and 34LiF–49NaF–15BeF_2 (mol%) mixtures with an excess of free fluoride ion content, revealed no evidence of attack in either the hot or cold areas of the loop. However, a microscopic examination of specimens removed from the cooler coil did reveal the presence of a small amount of metallic deposit. These studies (see **Table 5**) included (1) compatibility tests

Table 6 Nickel–molybdenum alloys' mechanical properties

Alloy	*Specimens in the delivery condition, $T = 20\,°C$*			*Specimens after the corrosion tests, $T = 20\,°C$*		
	$\sigma_{0.2}$ (kg mm^{-2})	*σ_B (kg mm^{-2})*	*δ (%)*	*$\sigma_{0.2}$ (kg mm^{-2})*	*σ_B (kg mm^{-2})*	*δ (%)*
HN80M-VI	110.4	119	10.9	103.9	120.0	28.0
	110.1	121.7	10.6	90.0	103.0	22.4
	112.7	122.3	9.1	89.5	101.1	22.4
HN80MTY (EK-50)	40.3	73.5	57.2	39.6	76.9	56.0
	39.6	70.0	54.0	40.3	73.4	55.0
				39.6	76.0	55.2
MONICR	50.0	75.0	54	38.5	67.5	53
	52.5	78.5	51	36.3	62.5	39
	50.5	75.3	53	36.3	65.0	38

between Ni–Mo alloys and molten 15LiF–58NaF–27BeF_2 (mol%) salt in a natural convection loop with a measurement of redox potential; (2) the effect of PuF_3 addition in molten 15LiF–58NaF–27BeF_2 (mol%) salt on compatibility with Ni–Mo alloys; and (3) Te corrosion for molten 15LiF–58NaF–27BeF_2 (mol%) salt and Ni–Mo alloys in stressed and unloaded conditions with measurement of the redox potential. Three Hastelloy N-type modified alloys, particularly HN80M-VI with 1.5% Nb, HN80MTY with 1% Al, and MONICR[68] with about 2% Fe, were chosen for the study in the corrosion facilities (see **Tables 3** and **6**).

Results of a 1200 h loop corrosion experiment[69] with online redox potential measurement demonstrated that high-temperature operations with molten 15LiF–58NaF–27BeF_2 (mol%) salt are feasible using carefully purified molten salts and loop internals. In the established interval of salt redox potential, 1.25–1.33 V relative to a Be reference electrode, corrosion is characterized by uniform loss of weight with low rate from sample surfaces. Under such exposure, the salt contained less than (in mass %): Ni – 0.004; Fe – 0.002; Cr – 0.002. Specimens of HN80M-VI and HN80MTY alloys from the hot leg of the loop exposed at temperatures from 620 to 695 °C showed a uniform corrosion rate from 2 to 5 μm year^{-1}. For the MONICR alloy, this value was up to 20 μm year^{-1} (see **Figure 6**).

No significant change in corrosion behavior of material samples was found in the melt due to the presence of 0.5 mol% PuF_3 addition in 15LiF–58NaF–27BeF_2 (mol%) salt. Specimens of HN80M-VI from the loop exposed during 400 h at 650 °C showed a uniform corrosion rate of about 6 μm year^{-1}. Under such exposure, the salt contained about (in mass %): Ni – 0.008; Fe –0.002; Cr – 0.002. No traces of IGC were found for any specimen after loop tests, even in the melt with PuF_3 addition. Data from chemical analysis of the specimen's surface layer showed a decrease in chromium content by 10–20 μm.

Tellurium IGC testing of the Ni–Mo alloys,[69,70] without and under mechanical load (80 MPa), for the 15LiF–58NaF–27BeF_2 (mol%) melt under dynamic and static conditions was carried out at 700 °C with exposure times of 100, 250, and 400 h at 1.2 V system redox potential. Under stress exposure to tellurium in the 15LiF–58NaF–27BeF_2 melt, the depth of cracks for MONICR specimens reached 220 μm ($K > 10\,000$ pC μm cm^{-1}). For HN80M-VI specimens tested without stress, rather low IGC intensity was observed ($K = 690$ pC μm cm^{-1}). However, under stress, the intensity of the HN80M-VI alloy cracking increased more than twice and the crack depth reached 125 μm. HN80MTY alloy is the most resistant to tellurium IGC of the Ni–Mo alloys studied. The intensity of its cracking under stress is $K = 880$ pC μm cm^{-1} (twice as low as that of HN80M-VI alloy).

The effect on the resistance to tellurium corrosion of Nb, Al, Ti, Re, and Mn doping agents added to the HN80M-type alloy was also studied in the Li,Na,Be/F facility at the RRC-Kurchatov Institute.[70] It was shown that both Re and Y additions only slightly increased the alloy's resistance to tellurium cracking. The alloy doped with Nb alone significantly increased IGC resistance. Addition of Mn gave a significant increase in alloy resistance to tellurium IGC. Therefore, testing of alloys with various compositions of doping elements to enhance the alloy's resistance to tellurium IGC should be continued in a thermal convection loop with long exposure times.

Finally, as can be seen from the considerations above, new findings in the developments of Ni–Mo alloys for MSRs with fuel salt temperatures up to 750 °C shift the emphasis from alloys modified with titanium and rare earths to those modified with

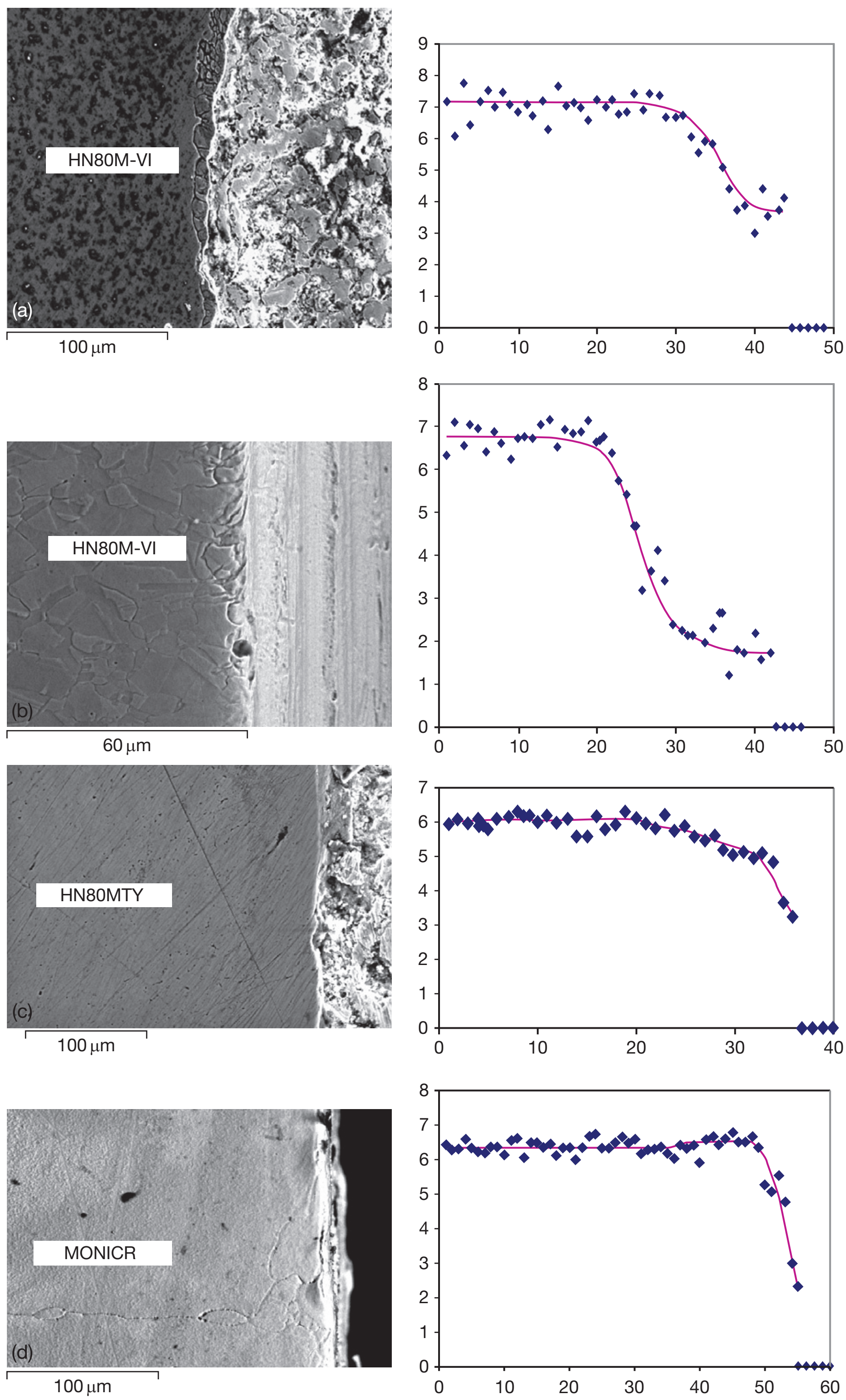

Figure 6 Chromium distribution (mass %) versus depth of the surface layer (μm) of specimens after corrosion tests in the loop: (a) quenched HN80M-VI, $T_{exposure}$ = 690 °C; (b) hot deformed HN80M-VI, $T_{exposure}$ = 670 °C; (c) quenched HN80MTY, $T_{exposure}$ = 620 °C; and (d) MONICR in the Scoda delivery state, $T_{exposure}$ = 690 °C. Reproduced from Ignatiev, V. V.; *et al. Nucl. Technol.* **2008**, *164*(1), 130–142.

niobium at ORNL[58] and aluminum at the RRC-Kurchatov Institute.[19] Subsequent steps for this type of metallic materials development must involve (1) irradiation, corrosion, tellurium exposure, mechanical property, and fabrication tests to finalize the composition for scale up; (2) procurement of large commercial heats of the reference alloy; (3) mechanical property and corrosion tests of at least 10 000 h duration; and (4) development of design methods and rules needed to design a reactor (breeder or burner) to be built of the modified alloy.

5.10.3.1.1.3 Alternative approaches

Certainly, some less mature approaches are possible and could be of interest for new MSR concepts. For example, Ni–W–Cr alloys have been recently proposed by Centre National de la Recherche Scientifique (CNRS) in France for their high potential to corrosion resistance for very high-temperature operation (>750 °C).[5] Temperatures >850 °C would require the use of new solutions such as refractory alloys or graphite. Included in further evaluation should also be the assessment of (1) new proposed solvent systems (e.g., Li,Th/F), (2) increased fuel salt outlet temperatures >750 °C, and (3) lower salt redox potentials from the point of view of establishing potentials that must be maintained to avoid IGC for Ni-base alloys.

5.10.3.1.2 Graphite for the core

Extensive prior work has demonstrated that graphite is compatible with molten fluoride salts (these are fundamental properties and are not particularly dependent on manufacturing). Much of the experience and data obtained in the gas-cooled reactor programs is directly applicable to MSRs. In particular, the limited lifetime of graphite resulted from neutron-induced damage. (See also **Chapter 4.10, Radiation Effects in Graphite**).

By the time the MSBR program at ORNL was cancelled in early 1973, the dimensional changes of graphite during irradiation had been studied for a number of years.[49,58] These changes depend largely on the degree of crystalline isotropy, but the volume changes fall into a rather consistent pattern. There is first a period of densification during which the volume decreases, and then a period of swelling in which the volume increases. The first period is of concern only because of the dimensional changes that occur, and the second period is of concern because of the dimensional changes and the formation of cracks. The formation of cracks would eventually allow salt to penetrate the graphite. The damage rate increases with increasing temperature, and hence, the graphite section size should be kept small enough to prevent temperatures in the graphite from exceeding those in the salt by a wide margin.

For fast neutron fluences greater than about 3×10^{22} neutrons cm^{-2} ($E_n > 50$ keV), the rate of graphite expansion becomes quite rapid, and it appears that this represents an upper limit to acceptable exposure of the graphite ($L \times P_m \approx 200$, where L is the moderator lifetime in full-power years and P_m is the maximum core power density in W cm^{-3}). For example, in the MSBR design, the maximum power density is about 70 W cm^{-3} and the useful graphite life would be about 3–4 years at full power.[16,17]

It was further required that the graphite be surface-sealed to prevent penetration of xenon into the graphite. Since replacement of the graphite would require considerable downtime, there was a strong incentive to increase the fluence limit of the graphite. A considerable part of the ORNL graphite program was spent in irradiating commercial graphites and samples of special graphites with potentially improved irradiation resistance. The approach taken to sealing the graphite was surface sealing with pyrocarbon. Because of the neutronic requirements, other substances could not be introduced in sufficient quantity to seal the surface.

Fission product gases, notably ^{135}Xe, will diffuse into graphite with some effect on neutron balance (poison fraction for uncoated graphite is about 0.01–0.02). It is desirable, especially for high flux cores, to hold Xe poisoning to the lowest possible level (poison fraction of 0.005). This requires graphites of very low permeability, for example, 10^{-8} cm^2 s^{-1}. The pyrolytic sealing work at ORNL was only partially successful. It was found that extreme care had to be taken to seal the material before irradiation. During irradiation, the injected pyrocarbon actually caused expansion to begin at lower fluences than those at which it would occur in the absence of the coating. Thus, the coating task was faced with a number of challenges.

The most detailed creep data exist on the US and German graphites for the HTR plant designs.[49] But these graphites, because of their coarse granularity and large pore size, are unsatisfactory for molten-salt applications. Fine-grained, isotropic, molded, or isostatically pressed, high-strength graphite suitable for core support structures (e.g., Carbone USA grade 2020 or Toyo Tanso grade IG-110[58] and Russian-made GSP type graphite[19]) is available today. Past experience has also demonstrated techniques for accommodating any radiation-induced dimensional changes in the graphite reactor vessel insulation. Development of sealing techniques should continue both with the pulse-impregnation technique and isotropic pyrolytic coatings applied at somewhat higher temperatures.

With relaxed requirements for breeding performance in the new wave of MSR concepts relative to the MSBR, the requirements for graphite would be diminished.[58] First, the lower gas permeability requirements mean that graphite damage limits can be raised. Second, if the salt flow rate through the core is decreased from the turbulent regime down to laminar one, the salt film at the graphite surface may offer sufficient resistance to xenon diffusion so that it will not be necessary to seal the graphite. Finally, the peak neutron flux at the graphite location can be reduced to levels such that the graphite will last for the lifetime of the reactor. As noted above, the lifetime criterion adopted for the breeder was that the allowable fluence would be about 3×10^{22} neutrons cm^{-2}. This was estimated to be the fluence at which the structure in advanced graphites would contain sufficient cracks to be permeable to xenon.

Experience has shown that, even at volume changes of about 10%, the graphite is not cracked but is uniformly dilated. For some nonbreeder devices where xenon permeability will not be of concern, the limit will be established by the formation of cracks sufficiently large for salt intrusion. It is likely that current technology graphites could be used to 3×10^{22} neutrons cm^{-2} and that improved graphites with a limit of 4×10^{22} neutrons cm^{-2} could be developed. Also, early efforts show promise that graphites with improved dimensional stability can be developed.

Finally, for nonmoderated MSR concepts (e.g., MSFR and MOSART) with a graphite reflector, there is no strong requirement on gas permeability ($10^{-8}\ cm^2\ s^{-1}$), but molten salt should be excluded from the open pore volume (pore structure $< 10^{-6}$ m). The last requirement can be met by currently available commercial graphite (See also **Chapter 4.10, Radiation Effects in Graphite**).

5.10.3.1.3 Materials for molten-salt fuel reprocessing system

For most established MSR concepts, processes involving (1) removal of uranium from fuel salt by fluorination and (2) selective extraction of transuranium elements and fission products from fuel salt into liquid bismuth are considered the most promising methods available. The material considerations below are oriented in these directions.

Nickel or nickel-base alloys can be used for the construction of fluorinators and containment of F_2, UF_6, and HF, though these metals would require protection by a frozen layer of fuel solvent over areas where contamination of the molten stream by the otherwise inevitable corrosion products would be severe. Many years of experience in fabrication and joining of such alloys have been accumulated[17,49] in the construction of reactors and associated engineering hardware. The corrosion of L nickel (low-carbon nickel with: 99.36% Ni; 0.02% C; 0.26% Fe; 0.06% Cu; 0.26% Mn; 0.04% Si; 0.001% S) and its alloys in the severe environment represented by fluorination of UF_6 from molten salts has been studied in some detail.[72] Most of the data were obtained during operation of two plant-scale fluorinators constructed of L nickel at temperatures ranging from 540 to 730 °C. A number of corrosion specimens (20 different materials) were located in the fluorinators. Several specimens, including INOR-1, had lower rates of maximum corrosive attack than L nickel.[72,73]

Nevertheless, L nickel, protected where necessary by frozen salt, is the preferred material for the fluorination–UF_6 absorption system since the other alloys would contribute volatile fluorides of chromium and molybdenum to the gaseous UF_6.

Absorption of UF_6 in molten salts containing UF_4 is proposed as the initial step in fuel reconstitution for many Th–U MSR concepts. The resulting solution, containing a significant concentration of UF_5, is quite corrosive. In principle, and perhaps in practice, the frozen salt protective layer could be used with vessels of nickel. It has been shown[74,75] that gold is a satisfactory container in small-scale experiments, and plans to use this expensive, but easily fabricable, metal in engineering-scale tests have been described.[76]

Most of the essential separations required of the processing plant are accomplished by selectively extracting species from salt streams into bismuth–lithium alloys or vice versa. Moreover, no satisfactory alternative to the selective extraction metal transfer process for removal of rare-earth fission products has been identified (reductive extraction from molten-salt fluoride mixtures into lithium–bismuth alloys).[58] These extractions pose difficult materials problems. Materials for containment of bismuth and its alloys are known, as are materials for containment of molten salts. Unfortunately, the two groups have few common members.

Carbon steels are not really satisfactory long-term containers for molten fluorides.[77,78] Nickel-base alloys are known[17,49] to be inadequate containers for bismuth.

Corrosion studies[79,80] showed molybdenum to resist attack by bismuth and to have no appreciable mass transfer at 500–700 °C for periods up to 10 000 h. Moreover, molybdenum is known to have excellent resistance to molten fluorides.[17,49] The external environment could be inert gas, but the problems in fabricating molybdenum are huge.

The resistance of tantalum and its alloys to molten fluorides has long been questioned, but no definitive tests had been made when previous surveys were written.[17,49] Further tests are obviously necessary, but continued satisfactory operation of the Ta–16% W loop with fuel salts must be considered encouraging. Pure tantalum and some of its alloys with tungsten (in particular, T-111 alloy: 8% W, 2% Hf, balance Ta) have been shown to be usefully compatible with molten bismuth and bismuth–lithium alloys. Tantalum is easy to fabricate, but the external environment must be a high vacuum.[58]

Graphite, which has excellent compatibility with fuel salt, also shows promise for the containment of bismuth. Compatibility tests to date have shown no evidence of chemical interaction between graphite and bismuth containing up to 3 wt% (50 at.%) lithium. However, the largest open pores of most commercially available polycrystalline graphites are penetrated to some extent by liquid bismuth. Capsule tests[81] of three commercial graphites (ATJ, AXF-5QBG, and Graphitite A) were conducted for 500 h at 700 °C using both high-purity bismuth and bismuth–3 mass % lithium. Although penetration by pure bismuth was negligible, the addition of lithium to the bismuth appeared to increase the depth of permeation and presumably altered the wetting characteristics of the bismuth. Limited penetration of graphite by bismuth solutions may be tolerable. If not, several approaches have the potential for decreasing the extent to which a porous graphite is penetrated by bismuth and bismuth–lithium alloys. Two well-established approaches are multiple impregnations with liquid hydrocarbons, which are then carbonized and/or graphitized, and pyrocarbon coatings. Graphite can be adequately protected at the outside with an inert gas, but it is difficult to fabricate into complex shapes.

As the chemistry of the processing system is engineered further through pilot plants, the precise type of hardware needed will be better defined. Significant additional research and development will necessarily be concerned with detailed tests of material compatibility and studies of welding, brazing, and other joining techniques, as well as joint design. Facilities for static testing, operation of thermal convection loop assemblies, and fabrication and operation of forced convection (pumped) loops will be required, along with sophisticated equipment for welding, brazing, etc., under carefully controlled atmospheres. Such facilities have been used routinely in the past and involve little, if any, additional development.

5.10.4 Advanced High-Temperature Reactor

When considering materials performance in the AHTR,[82] the materials can be classified into three main categories: (1) graphite and C/C composites, (2) low-pressure reactor vessel materials, and (3) high-temperature metallic components.

The graphite core, reflector and vessel insulation, and C/C composite core supports and control rods will operate in a molten-salt environment over a range of temperatures from 500 to 1100 °C or higher (peak temperature being selected as a trade-off between reactor thermal inertia, thermal blanket system performance, and material properties). It is anticipated that, for the AHTR, properly designed and manufactured C/C composite structures will demonstrate similarly good properties in the presence of molten fluoride salts and better mechanical properties.

The reactor vessel materials[3] must be capable for operation at 500 °C and may need to withstand temperature excursions to 800 °C for 100 h under accident conditions. The vessel must demonstrate adequate strength and creep resistance (long-term and short-term), good thermal-aging properties, low-irradiation degradation, fabricability, good corrosion resistance, and the ability to develop and maintain a high-emissivity surface in air. As previously noted, nickel-base alloys demonstrate good corrosion resistance to molten salts. Therefore, ORNL proposed[82] that stable, high-strength, high-temperature materials, such as 9Cr–1MoV, be coated with a high-nickel coat for the reactor vessel application. Should the vessel be required to withstand excessive off normal temperatures, base materials such as 304L, 316L, 347, Alloy 800H, or HT may be appropriate. In addition, monolithic materials with adequate corrosion resistance to molten fluoride salts and high-temperature strength may include Alloy 800H or HT, Hastelloy N, and Haynes 242. Performance of the suggested materials needs to be evaluated, especially at higher temperatures. Further, the ability to develop and maintain a high-emissivity layer on the surface of the vessel exposed to argon or air must be demonstrated, but this is not considered a major barrier.

High-temperature metallic or composite materials are needed for use up to 1000 °C in the presence of molten fluoride salts on one side and an insulation system in contact with air on the other side. Piping and heat exchangers are examples for the latter conditions. Pumps and other components submerged below the primary salt pool will need to survive higher temperatures for short times or be replaceable at reasonable expense. The metallic materials used in these environments must demonstrate adequate strength (long-term and short-term), good thermal-aging properties, low-irradiation degradation, fabricability, and good corrosion resistance. Based on material maturity and the need for high nickel for fluoride corrosion resistance, stable, high-strength, high-temperature metallic materials such as Inconel 617, Haynes 230, Alloy 800H, Hastelloy X or XR, VDM 602CA, and HP modified with a coating with high-nickel content could be possible candidates for detailed evaluation.[3,26] Should higher temperature alloys be required, Haynes 214, cast Ni-base superalloys (for pumps), and ODS MA 754 are possible candidates. Recent experience suggests that, should the oxidation potential of the salt be made very reducing, it may be possible to use ODS MA 956 (an iron-base alloy). These monolithic materials will require more testing and data development. For composite materials, liquid-silicon-impregnated (LSI) composites, with chemical vapor deposition carbon coatings, may be promising for use for pumps, piping, and heat exchangers.[3] LSI composites have several potentially attractive features, including the ability to maintain nearly full mechanical strength to temperatures approaching 1400 °C, inexpensive and commercially available fabrication materials, and the capability for simple machining and joining of carbon–carbon performs, allowing the fabrication of highly complex component geometries.

As already discussed, corrosion activity of molten salts is dependent upon the major salt constituents and impurities in the salt. The coolant salt can be prepared and maintained in such a way that impurities do not control the corrosion response. It is expected that coolant salts can be used at significantly higher temperatures than were established in the MSR design because of the different corrosion characteristics of a clean salt coolant versus a molten salt-containing actinides and fission product fluorides. A wider range of material options also exists. The presence of uranium dissolved in the salt was always found to accelerate corrosion, and there exist additional methods to prevent corrosion when uranium is not present in the salt.

The equilibrium level of dissolved chromium has been measured for fuel salts, but not for coolant salts.[83–85] Although information on fuel salts is not directly applicable to coolants, it is expected that fuel solvents that experience minimal corrosion would also be better coolants.[26] Review of dissolved chromium levels for various fuel salts again reveals that the molten 46.5LiF–11.5NaF–42KF (in mol%) mixture stands somewhat apart from the other salts as it sustains a higher degree of corrosion. It also appears that there is some benefit in avoiding a very acidic (high ZrF_4 or BeF_2 content) system and that a salt mixture that has a nearly complete coordination shell (2:1 ratio of alkali halide to Zr or Be and heavier alkali salt) has the least potential for supporting corrosion based on temperature sensitivities. This approach is a significant oversimplification, as the identity of the various species is very important. For example, the saturating species that contain chromium are different for each of these salts.

Although <10% of all corrosion testing was done with salts that were free of uranium, this small fraction amounts to a significant body of work because of the extensive test program carried out. The results of testing for uranium-free salts reveals that Hastelloy N (INOR-8), just as it is for fuel salts (see previous section), is a superior choice (rather than Inconel or stainless steels) for coolant salts. The corrosion is so intense and the duration so short for most Inconel tests that it is hard to make a judgment about which salt is the least susceptible to corrosion.

For Hastelloy N loops at temperatures up to 700 °C, the corrosion is so minor that it is hard to sort out corrosion effects due to the salt composition. Again, a molten 46.5LiF–11.5NaF–42KF (in mol%) mixture is among the worst. Some additional Inconel loop tests[86,87] were conducted with special fuel salt mixtures in which the ZrF_4 and BeF_2 concentrations were varied in an attempt to select the best composition. However, these tests were somewhat inconclusive because of the short test duration (500 h) and impurity effects. Within the resolution of these tests, the following trends were verified: very basic (FLiNaK) and very acidic (LiF–ZrF_4) salts showed the worst performance.[26]

Corrosion tests of Hastelloy N, Hastelloy X, Haynes-230, Inconel-617, and Incoloy-800H at a high temperature of 850 °C were performed at the US University of Wisconsin-Madison in a molten 46.5LiF–11.5NaF–42KF (in mol%) mixture, with the goal of ranking alloy suitability for the AHTR core.[88] In particular, an attempt was made to simulate material performance in the corrosion system with a primary salt coolant, metal reactor vessel, and graphite fuel materials. The isothermal tests were performed for 500 h in sealed graphite crucibles under an argon cover gas, without any redox measurement and control strategy. Certainly, graphite crucibles may accelerate the corrosion process by promoting the formation of carbide phases on the walls of the test crucibles, but they did not alter the basic corrosion mechanism. Corrosion was noted to occur predominantly by release of Cr from the alloys, an effect that was particularly pronounced at the grain boundaries of these alloys. Mass loss due to corrosion generally correlated with the initial Cr content of the alloys, and was consistent with the Cr content measured in the salts after corrosion tests. The corrosion attack was more severe for Hastelloy N (6.3% Cr), where Cr depletion up to depths of about 50 μm was observed. Hastelloy X (21.3% Cr) exhibited grain boundary attack up to depths of at least 300 μm below the surface. Inconel-617 (22.1% Cr) was uniformly depleted in Cr up to depths of about 100 μm from the surface and experienced dramatic grain boundary corrosion throughout the thickness of the sample. Similar attack was observed for Haynes-230 (22.5% Cr); however, the surface of Haynes-230 exhibited a Ni-enriched layer. For Haynes-230, W-rich precipitates were observed at the grain boundaries due to the relatively high W content of this alloy, demonstrating that W, like Mo, is resistant to attack from molten fluoride salt. The fundamental reason why Haynes-230 experienced more weight loss than the other high Cr-containing alloys needs further investigation. Two Cr-free alloys, Ni-201 and Nb–1Zr, were also tested. Ni-201, a nearly pure Ni alloy with minor alloying additions, exhibited good resistance to corrosion, whereas Nb–1Zr alloy exhibited extensive corrosion attack.

At various periods at ORNL, control of the oxidation–reduction state of the salt was explored as a means to minimize corrosion. However, it was not practical, because strong reductants either reduced zirconium or uranium in the salt to a metal that plated on the alloy wall or resulted in some other undesirable phase segregation. During the MSRE operation, periodic adjustment of the U(III)/U(IV) ratio was effective in limiting corrosion in the fuel circuit. Keiser[89] also explored the possibility of using metallic beryllium to reduce corrosion in stainless steel containing a $LiF–BeF_2$ salt, where the oxidation potential of the salt could be lowered by buffering with metallic beryllium without concerns for disproportionation of uranium trifluoride; the corrosion rate was decreased at 650 °C from 8 to 2 μm year^{-1}.

This treatment was effective only as long as the metallic beryllium was immersed in the salt. There was little, if any, buffering capacity in this salt to maintain the reducing environment throughout the melt. Del Cul *et al.*[90] have identified and tested candidate agents that could be used as redox buffers to maintain a reducing environment in the coolant circuit. None of these redox-control strategies has been developed to the extent that we can rely on them for a definite salt selection. However, some useful observations can be made in this regard. For a lower temperature system (<750 °C), it appears that Hastelloy N is fully capable of serving as a containment alloy without the need for a sophisticated redox strategy. Even an alkali fluoride, such as a molten 46.5LiF–11.5NaF–42KF (in mol%) mixture, could be suitable. For temperatures in excess of 750 °C and for alloys that contain more chromium (as most higher temperature alloys do), it appears that a reducing salt will be needed to minimize corrosion. Inconel without the benefit of a reducing environment was found to be unsuitable for long-term use. Only a mildly reducing environment is possible with a ZrF_4-containing salt, since a strongly reducing redox potential would reduce ZrF_4 itself. Much more reducing systems can be devised with either LiF–NaF–KF- or BeF_2-containing salts. Some very important material compatibility issues will have to be explored in order to use a highly reducing salt at these higher temperatures because events such as carbide formation and carburization/decarburization of the alloy (not discussed in the report) become a significant threat. Should low-chromium/chromium-free alloys or suitable clad systems be devised as a container, these problems with salt selection will largely disappear. However, in the absence of this solution, ORNL has considered two strategies: (1) select a salt that should support the minimum level of corrosion in the absence of a highly reducing environment (some ZrF_4 salts, BeF_2-containing salts) or (2) select a salt with a large redox window that can be maintained in a highly reducing state (LiF–NaF–KF- or BeF_2-containing salts). Given the expense and difficulty of carrying out development work with beryllium-containing salts, ORNL proposed to explore the most promising ZrF_4 salts without strong reductants and to explore LiF–NaF–KF with strong reductants and/or redox buffers.[26]

5.10.5 Liquid-Salt-Cooled Fast Reactor

There are no metallic components in the reference MSR core. While Hastelloy N or another nickel-base alloy is suitable for the reactor vessel, heat exchangers, pumps, main circulation pipes, drain tanks, and other equipment, it may not be suitable for LSFR in-core components (structure and fuel cladding), which will be subjected to higher temperatures and receive large fast neutron fluences in the core. The metal in-core components are likely to be the primary technical challenge for an LSFR, given the requirements for higher temperature service, resistance to neutron radiation damage, and corrosion resistance to liquid salts. The use of binary metallic materials (either clad or coated) may be desirable for some applications (including the reactor vessel), in order to confer appropriate strength and corrosion resistance.

Generally, practical metal systems are based on (1) nickel-, (2) iron-, or (3) molybdenum-base alloys.[3]

The nickel-base alloys for high-temperature service in molten-salt coolants (but not as in-core components) have been evaluated as part of the AHTR research and development activities (see previous section). Some of these alloys are known to have excellent chemical compatibility with molten salt-coolants; however, there is mixed experience with the irradiation performance of nickel alloys. For a UK Prototype Fast Reactor experience[91,92] with PE-16 irradiation performance, a nickel alloy (17Cr, 43Ni, 3Mo, 2.5Ti, 34Fe + Al, in mass %) was good, but at lower temperatures than required for LSFRs. At the same time, many nickel-base super alloys have poor radiation stability (grain boundary embrittlement). The potential of nickel-base alloys at the higher temperatures for use in an LSFR core spectrum is not well understood. The strength of many nickel alloys is a consequence of nickel–silicon precipitates. In irradiation fields, these precipitates can dissolve, with the silicon migrating to the grain boundaries and causing the alloy to weaken. For these alloys, it may be feasible to overcome this difficulty by the development of oxide-dispersion-system (ODS) nickel alloys. However, only very limited work has been done on these systems.

The iron-base alloys have good radiation resistance. The primary LSFR concern associated with iron alloys is their long-term high-temperature corrosion resistance. Some of these alloys are known to have excellent chemical compatibility with molten-salt coolants.

For example, static corrosion tests[87] were performed recently in molten 46.5LiF–11.5NaF–42KF and 66LiF–34BeF_2 (in mol%) mixtures at 500 and 600 °C for 1000 h. The purpose was to study the corrosion characteristics of reduced-activation ferritic steels, JLF-1 (8.92Cr–2W) in the molten salts. The concentration of HF in the melts was measured by the slurry pH titration method before and after exposure. The HF concentration determined the fluoridation potential. The corrosion was mainly caused by dissolution of iron and chromium in the melts due to fluoridation and/or electrochemical corrosion. The corrosion depth of the specimens at 600 °C, which was obtained from the weight losses, was 0.637 μm in 66LiF–34BeF_2 melt and 6.73 μm in 46.5LiF–11.5NaF–42KF melt. The corrosion rate of SS304 and SS316L steels in 66LiF–34BeF_2 melt after 1000 h exposure at 600 °C was estimated as 10.6 and 5.4 μm $year^{-1}$, respectively.

Russian experience[20] with molten-salt fluorides and AP-164 iron-base alloy (14–16 Cr, 22–25 Ni, 0.5–1 Mn, 4–5 W, 1.4–1.8 Ti, 0.08 C, in mass %) was good, but also at lower temperatures (630 °C) than required for LSFRs (700–750 °C).

To overcome the temperature limitations on iron-base systems, there has been significant developmental work on ODS iron alloys for fast reactors.[93] These alloys contain rare-earth oxides, such as yttrium oxide, that enable iron alloys to maintain strength at up to 80% of their melting point versus 50% for traditional alloys. The limited corrosion testing of iron-base alloys in molten fluoride salt coolants indicates the potential for corrosion-resistant iron-base systems. However, more corrosion testing will be required to expand upper operating temperature to 700–750 °C before gaining more confidence in such an approach.

Molybdenum alloys are compatible with molten salts and have good thermophysical properties.[94] Molybdenum has a very high melting point (2600 °C), high thermal conductivity, and moderate thermal neutron cross-section (2.65 barns). However, isotopically separated molybdenum,[94] with its very low nuclear cross-section, is an option. There are significant challenges with molybdenum alloys: (1) such alloys are difficult to weld, (2) the fracture toughness is somewhat low with concerns about radiation embrittlement, and (3) high-temperature oxidizing conditions must be avoided because MoO_3 has a melting temperature of 795 °C. The potential oxidation should not be a significant concern for an LSFR because the molten-salt mixture (such as sodium) will be subjected to chemically reducing conditions. The fracture toughness is a primary concern at lower temperatures. Radiation damage is temperature dependent and is minimized by operating at higher temperatures in the range from 650 to 1000 °C. Molybdenum-base alloys may ultimately allow the construction of a very high-temperature LSFR and is a class of materials where higher temperatures improve material properties.

5.10.6 Secondary Circuit Coolants

In the secondary circuits of an MSR, AHTR, LSFR, or SFR, the main difference compared to the primary one for the container metal will be the absence of fission products and uranium in the coolant salt and the much lower neutron fluences. This material must have moderate oxidation resistance and must resist corrosion by salt not containing fission products or uranium. The corrosion for molten fluoride salts was discussed in detail in previous sections. Very little corrosion data are available for nuclear application of molten-salt mixtures, including nitrate, chloride, and fluoroborate salts, than for molten fluoride salts, especially for temperatures above 600 °C.

A nitrate mixture of $60NaN0_3$–$40KNO_3$ (in mass %) has been proposed for use in the intermediate circuit of SFRs and LSFRs.[2] This molten-salt mixture is attractive for such applications because of its high heat capacity, its low reactivity in the event of a leak to air or steam, and the low operating pressures required for its use. However, the feasibility of such a system depends partly on the compatibility of the salt with candidate structural alloys. Alloy 800 and types 304, 304L, and 316SS were exposed in a natural convection loop filled with molten $NaNO_3$–KNO_3 salt in the temperature range 375–600 °C for more than 4500 h.[7] The weight change data for the alloys indicated that (1) the metal in the oxide film constituted most of the metal loss; (2) the corrosion rate, in general, increased with temperature; and (3) although the greatest metal loss corresponded to a penetration rate of 25 $\mu m\,year^{-1}$, the rate was <13 $\mu m\,year^{-1}$ in most cases. Spallation had a significant effect on metal loss at intermediate temperatures in the type 304L stainless steel loop. Metallographic examinations showed no evidence of intergranular attack. The exposure resulted in the growth of thin oxide films on significant cold-leg deposits. Weight change data further confirmed the absence of thermal gradient mass transport processes in these draw salt systems. Raising the maximum temperature of the type 316SS loop from 595 to 620 °C dramatically increased the corrosion rate, and it appears that 600 °C may be the limiting temperature for use of such alloys in draw salt.

Material corrosion resistance for the SFR intermediate circuit containing 56LiCl–44LiOH (in mol%) was studied in Russia.[20] The corrosion facility was constructed according to a three-loop scheme. The first circuit was filled with sodium to a maximum temperature of 530 °C. The second (intermediate) circuit was filled with a molten 56LiCl–44LiOH mixture, which was heated from sodium to a maximum temperature of 490 °C. The last circuit with a steam generator was cooled down to 430 °C. The loop structural material was stainless steel 10H18N10T, with the exception of the sodium-salt heat exchanger and steam generator, which were made of a perlite 10H2M steel. Specimens of 10H2M (Fe–2% Cr–1% Mo–0.1% C), 10H18N10T, H9MFB (Fe–9% Cr–1% Mo–1% V–1% Nb), 08H14MF (Fe–14% Cr–1% Mo–1% V–0.08% C), 10H14GMFB (Fe–14% Cr–1% Mn–1% Mo–1% V–1% Nb), and 10H14N5MF (Fe–14% Cr–5% Ni–1% Mo–1% V) steels for corrosion tests were inserted correspondingly in the hot and cold legs of the loops. The specimen in the molten-salt loop was held for a little over 2000 h. The highest corrosion resistance was displayed by steels 10H18N10T and 10H14GFB, and the least by 10H2M. The 10H18N10T steel uniform corrosion rate in the molten 56LiCl–44LiOH mixture was 50 $\mu m\,year^{-1}$. The metallographic study also determined that 10H18N10T steel corrosion had an intergranular character (crack depth up to 60 $\mu m\,year^{-1}$). However, it should be noted here that according to chemical analysis data, the initial salt composition contained about 1% H_2O. Also, corrosion product deposits were found in some local sections of the molten-salt loop.

For the purpose of comparison, the most relevant corrosion results for chloride salts are displayed in Table 7.[95] These results do not conform to any expected or predictable trends. For example, the effect of chromium content in the alloy does not seem to be an important factor, and the effect of temperature is not clear. Unexpected variability in the tests very likely reflects variation in the purity of the starting materials and the degree to which impurities were excluded from the loop during operation. The corrosion rates are rather high for these salts at a relatively low temperature (~550 °C). These rates are similar to those experienced with fluoride salts

Table 7 Summary of Brookhaven loop corrosion tests for chloride salts

Loop[a]	*Loop material*	*%Cr–Ni–Mo in Fe alloy*	*Duration (h)*	T_{max} *(°C)*	ΔT *(°C)*	*Corrosion rate (µm year⁻¹)*
Tests with LiCl–KCl eutectic salt						
TCL-F	347SS	17.5–1.4–0.2	5500	575	155	12
TCL-L1	410SS	12.4–0.2–0.1	2200	570	160	50
TCL-L3	2.25Cr–1Mo	2.25–0–1	697	550	150	High[b]
Tests with 30NaCl–20KCl–50MgCl$_2$ eutectic salt (mol%)						
TCL-L5	347SS	17.5–11.4–0.2	2467	500	45	93
TCL-L6	410SS	12.4–0.2–0.1	3971	494	42	79
FCL-M1	347SS	17.5–11.4–0.2	1034	520	0	31
FCL-M2	347SS	17.5–11.4–0.2	656	515	0	256

[a]TCL refers to thermal convection loop, FCL refers to a forced convection loop.
[b]No specimen corrosion depth was reported, but salt analysis showed 0.11% iron.
Source: Susskind, H.; *et al.* Corrosion studies for a fused salt-liquid metal extraction process for the liquid metal fuel reactor, BNL-585; Brookhaven National Laboratory: Brookhaven, NY, 1960

Table 8 Summary of Hastelloy N corrosion loops with 8NaF–92NaBF$_4$ salt at ORNL

Loop	*Duration (h)*	T_{max} *(°C)*	ΔT *(°C)*	*Corrosion rate (µm year⁻¹)*
NCL-13A	30.627	607	125	16
NCL-14	39.202	607	150	13
NCL-17	24.865	607	100	24
NCL-20	19.928	688	250	24
FCL-1	17.000	621	167	29
FCL-2	5.300	621	167	23

Source: Bamberger, C. E.; Baes, C. F. Corrosion of Hastelloy N by fluoroborate melts, ORNL-4832; ORNL: Oak Ridge, TN, 1973; pp 44–45.

in contact with stainless steels and Inconel at ~800 °C and are much higher than those experienced with Hastelloy N in contact with fluoride salts at temperatures as high as 815 °C.

The corrosion database for fluoroborates is shown in Table 8.[45] Improvement in fluoroborate salt purity during the MSBR program was responsible for a steadily decreasing level of corrosion in tests. For NaF–NaBF$_4$ secondary coolant, ORNL data[45] in thermal corrosion loops containing Hastelloy N specimens lie in the interval of 5–20 µm year^{-1} and are determined mostly by the degree of salt purification. These data are in good agreement with later RRC-Kurchatov Institute corrosion studies[20] for Russian nickel-base alloy of the HN80MT type (about 10–15 µm year^{-1} at 600 °C). The ORNL experience reveals that the coolant fluoroborate salt absorbs moisture quite readily with attendant generalized corrosion. On occasions when leaks developed, the corrosion rate had increased and then decreased as the impurities were exhausted. During these periods of high corrosion, all components of the alloy were removed uniformly from the hot leg and deposited in the cold leg. Crystals of Na$_3$CrF$_6$ deposited in the cold regions as its solubility was exceeded.

In summing up the results of work on secondary circuit coolants, it should be emphasized that, among the presently known high-temperature energy carriers with operating temperatures ranging from 300 to 550 °C, the most promising for practical utilization is nitrate–nitrite molten-salt mixtures. As for the range of higher operating temperatures >700 °C, there are some alternatives with different maturity. The database exists for fluoride-containing tests in the 800–900 °C temperature range with both Inconel and Hastelloy N (INOR-8) alloys. No experience exists with loop corrosion tests using chlorides or fluoroborates at temperatures approaching the levels anticipated in the loop that transports heat from the AHTR or VHTR nuclear plant to the hydrogen production plant. There is a need to demonstrate and recommend an improved method for purification of chloride and fluoroborate salts to be used in corrosion tests.[26,34] This new method should become a purification standard to be used in conjunction with corrosion tests. High-temperature corrosion tests with properly purified chloride salts should be conducted to confirm the possibility of using chloride and fluoroborate salts in the loop that will transport heat from the AHTR or VHTR nuclear plant to the hydrogen production plant. These tests should include both batch exposures and loop tests and will probably also require the innovative use of redox buffers to minimize corrosion.[26,34]

References

1. Ignatiev, V.; Feynberg, O.; Smirnov, V.; Tataurov, A.; Vanukova, G.; Zakirov, R. Characteristics of molten salt actinide recycler and transmuter system. In *Proceedings of International Conference on Emerging Nuclear Energy Systems*, Brussels, Belgium, Aug 21–26, 2005; paper ICQ064.
2. Forsberg, C. W.; Lebrun, C.; Merlet-Lucotte, E.; Renault, C.; Ignatiev, V. *Revue Generale Nucleaire* **2007**, *4*, 63–71.
3. Forsberg, C. W.; *et al.* Design options for the advanced high-temperature reactor. In *Proceedings of International Congress on Advances in Nuclear Power Plants*, Anaheim, CA, Jun 8–12, 2008.
4. Delpech, S.; *et al. J. Fluorine Chem.* **2009**, *130*(1), 11–17.
5. Renault, C.; *et al.* European molten salt reactor. In *Proceedings of Seventh European Commission Conference on Euroatom Research and Training in Reactor System*s, Prague, Czech Republic, Jun 22–24, 2009.
6. Chechetkin, A. V. *High Temperature Coolants*; Gosenergoizdat: Moscow, USSR, 1962.
7. Tortorelli, P. F.; DeVan, J. H. Thermal convection loop study of the corrosion of Fe–Ni–Cr alloys by molten $NaNO_3$–KNO_3, ORNL/TM-8298; ORNL: Oak Ridge, TN, 1982.
8. Mar, R. W.; *et al.* The use of molten nitrate salts in high temperature energy conversion systems. In *Proceedings of First International Symposium on Molten Salt Chemistry and Technology*, Kyoto, Japan, Apr 20–22, 1983; pp 285–288.
9. Taube, M. *Fast Reactors Using Molten Chloride Salts as Fuel*; Wurenlingen: Switzerland, 1978.
10. Migai, L. L.; Taritsina, T. A. *Corrosion Resistance of Structural Materials in Halides and their Mixtures*. Moscow, USSR: Metallurgy, 1988.
11. Rosenthal, M. W.; *et al. Nucl. Appl. Technol.* **1970**, *8*(2), 107–118.
12. Bettis, E. S.; *et al. Nucl. Sci. Eng.* **1957**, *2*(6), 804–812.
13. Manly, W. D.; *et al.* ARE-metallurgical aspects, ORNL-2349; ORNL: Oak Ridge, TN, 1957.
14. Cottrell, W. B. Disassembly and postoperative examination of the aircraft reactor experiment, ORNL-1868; ORNL: Oak Ridge, TN, 1958.
15. Haubenreich, P. N.; Engel, J. R. *Nucl. Appl. Technol.* **1970**, *8*(2), 107–140.
16. Bettis, E. S.; Robertson, R. C. *Nucl. Appl. Technol.* **1970**, *8* (2), 190.
17. Rosenthal, M. W.; Haubenreich, P. N.; Briggs, R. B. Development status of molten salt breeder reactors, ORNL-4812; ORNL: Oak Ridge, TN, 1972; p 250.
18. Furukava, K.; *et al. J. Nucl. Sci. Technol.* **1990**, *27*, 1157–1178.
19. Novikov, V. M.; Ignatiev, V. V.; Fedulov, V. I.; Cherednikov, V. N. *Molten Salt Reactors: Perspectives and Problems*; Energoatomizdat: Moscow, USSR, 1990.
20. Ignatiev, V. V.; Novikov, V. M.; Surenkov, A. I.; Fedulov, V. I. The state of the problem on materials as applied to molten-salt reactor: Problems and ways of solution, Preprint IAE-5678/11; Institute of Atomic Energy: Moscow, USSR, 1993.
21. Grope detravail CEA–EDF. Materiax metalliques RSF: Synfese des etudes realisees entre 1973 et 1983, Rapport EDF HT/12/77/83; dossier materiax metalliques: Paris, France, 1983.
22. Lecarpentier, D.; Vergnes, J. *Nucl. Eng. Des.* **2002**, *216*, 43–67.
23. Forsberg, C. W.; Peterson, P. F.; Pickard, P. S. *Nucl. Technol.* **2003**, *144*, 289–302.
24. Forsberg, C. W.; *et al.* Practical aspects of liquid-salt-cooled fast-neutron reactors. In *Proceedings of ICAPP'05*, Seoul, Korea, May 15–19, 2005, paper 5643.
25. Petroski, R.; Hejzlar, P.; Todreas, N. E. *Nucl. Eng. Des*. **2009**, doi:10.1016/j.nucengdes.2009.07.012.
26. Williams, D. F.; Toth, L. M.; Clarno, K. T. Assessment of candidate molten salt coolants for the advanced high-temperature reactor, ORNL/TM-2006/12; ORNL: Oak Ridge, TN, 2006.
27. Thoma, R. E. Ed. Phase diagrams of nuclear reactor materials, ORNL-2548; ORNL: Oak Ridge, TN, 1959.
28. Barton, C. J.; Strehlow, R. A. *J. Inorg. Nucl. Chem.* **1961**, *18*, 143.
29. Atomic Energy Commission. Molten salt breeder reactor concept; Quarterly report for period ending July 21, NP-19145; Bombay, India, 1971.
30. Bamberger, C. E.; Ross, R. S.; Baes, C. F. *J. Inorg. Nucl. Chem.* **1971**, *33*, 3591–3594.
31. Ward, W. T.; Strehlow, R. A.; Grimes, W. R.; Watson, G. M. *J. Chem. Eng.* **1960**, *5*(2), 137–142.
32. Barton, C. J. *J. Phys. Chem.* **1960**, *64*, 306–309.
33. Ignatiev, V.; Golovatov, Y.; Merzlyakov, A.; Panov, A.; Subbotin, V. *Atom. Energy* **2006**, *101*(5), 364–372.
34. Williams, D. F. Assessment of candidate molten salt coolants for the NGNP/NHI heat-transfer loop, ORNL/TM-2006/69; ORNL: Oak Ridge, TN, 2006.
35. Manly, W. D.; Richardson, L. S.; Vreeland, D. E. *Prog. Nucl. Energy* **1960**, *2*(4), 164–179.
36. DeVan, J. H.; Evans, R. B., III. Corrosion behavior of reactor materials in fluoride salt mixtures, ORNL/TM-328; ORNL: Oak Ridge, TN, 1962.
37. Adamson, G. M.; Crouse, R. S.; Manly, W. D. Interim report on corrosion by zirconium-base fluorides, ORNL-2338; ORNL: Oak Ridge, TN, 1961.
38. De Van, J. H.; Evans, R. B. In *Proceedings of the Conference on Corrosion of Reactor Materials*, Jun 4–8, 1962; IAEA: Vienna, Austria, 1962; pp 557–579.
39. Grimes, W. R. *Nucl. Appl. Technol.* **1970**, *8*(2), 137–155.
40. Baes, C. F. *J. Nucl. Mater.* **1974**, *51*(1), 149.
41. Evans, R. B., III; DeVan, J. H.; Watson, G. M. Self-diffusion of chromium in nickel-base alloys, ORNL-2982; ORNL: Oak Ridge, TN, 1960.
42. Koger, J. W. Alloy compatibility with LiF–BeF_2 salts containing ThF_4 and UF_4, ORNL-TM-4286; ORNL: Oak Ridge, TN, 1972.
43. Keiser, J. R.; *et al.* Salt corrosion studies, ORNL-5078; ORNL: Oak Ridge, TN, 1975; pp 91–97.
44. Koger, J. W. Forced-convection loop corrosion studies, Huntley WR and ORNL-4832; ORNL: Oak Ridge, TN, 1973; pp 135–137.
45. Bamberger, C. E.; Baes, C. F. Corrosion of Hastelloy N by fluoroborate melts, ORNL-4832; ORNL: Oak Ridge, TN, 1973; pp 44–45.
46. Keiser, J. R. Compatibility studies of potential molten-salt breeder reactor materials in molten fluoride salts, ORNL-TM-5783; ORNL: Oak Ridge, TN, 1977.
47. Ignatiev, V.; Fedulov, V.; Novikov, V.; Surenkov, A. *Voprocy Atomnoi Nauki i Tehkniki: Atomno – Vodorodnaya Energetika i Tehnologiya* **1981**, *3*(10), 74–76.
48. De Van, H.; Distefano, J. R.; Eartherly, W. P.; Keiser, J. R.; Klueh, R. L. Materials considerations for molten salt accelerator based plutonium conversion system. In *Proceedings of the Global'93 International Conference*, Las Vegas, 1993.

49. McNeese, L. E. Program plan for development of molten-salt breeder reactors, ORNL-5018; ORNL: Oak Ridge, TN, 1974; pp 5–46.
50. Maya, L. *J. Inorg. Chem.* **1976**, *15*(9), 2179–2184.
51. Mays, G. T. Distribution and behavior of tritium in the coolant-salt technology facility, ORNL/TM-5759; ORNL: Oak Ridge, TN, 1977.
52. Briggs, R. B. Molten salt reactor program semiannual progress report for period ending February 28, ORNL-3282; ORNL: Oak Ridge, TN, 1962.
53. Shaffer, J. H. Preparation of MSRE fuel, coolant and flush salt, ORNL-3708; ORNL: Oak Ridge, TN, 1964; pp 288–302.
54. Briggs, R. B. Molten salt reactor program semiannual progress report for period ending February 28, ORNL-3812; ORNL: Oak Ridge, TN, 1965; pp 121–168.
55. Shaffer, J. H. Preparation and handling of salt mixtures for the molten salt reactor experiment, ORNL-4616; ORNL: Oak Ridge, TN, 1971.
56. Cherginets, V. L. *Handbook of Solvents*; Chemical Technology: Toronto, Canada, 2001; Chap. 10.3, pp 633–635.
57. Cherginets, V. L.; Rebrova, T. P. *Electrochim. Acta* **1999**, *45*(3), 469–476.
58. Engel, J. R.; Bauman, H. F.; Dearing, J. F.; Grimes, W. R.; McCoy, E. H.; Rhoades, W. A. Development status and potential program for development of proliferation resistance molten salt reactor, ORNL-TM-6415; ORNL: Oak Ridge, TN, 1979.
59. Harries, O. R. *J. Br. Nucl. Soc.* **1966**, *5*, 74.
60. Mc Coy, H. E.; Roche, T. K. Post irradiation creep properties of modified Hastelloy N, ORNL-5078; ORNL: Oak Ridge, TN, 1975; pp 82–84.
61. Mc Coy, H. E.; *et al.* Intergranular cracking of structural materials exposed to fuel salt, ORNL-4782; ORNL: Oak Ridge, TN, 1972; pp 109–144.
62. Mc Coy, H. E.; *et al.* Intergranular cracking of structural materials exposed to fuel salt, ORNL-4832; ORNL: Oak Ridge, TN, 1972; pp 63–76.
63. Mc Coy, H. E.; *et al.* Metallographic examination of samples exposed to tellurium-containing environments, ORNL-5078; ORNL: Oak Ridge, TN, 1972; pp 108–113.
64. Mc Coy, H. E.; *et al.* Development of modified Hastelloy N, ORNL-5132; ORNL: Oak Ridge, TN, 1976; pp 42–162.
65. Mc Coy, H. E.; *et al.* Status of materials development for molten salt reactors, ORNL-TM-5920; ORNL: Oak Ridge, TN, 1978.
66. Keiser, J. R. Status of tellurium–Hastelloy N studies in molten fluoride salts, ORNL-TM-6002; ORNL: Oak Ridge, TN, 1977.
67. Ignatiev, V.; Fedulov, V.; Novikov, V.; Surenkov, A. *Voprocy Atomnoi Nauki i Tehkniki: Atomno – Vodorodnaya Energetika i Tehnologiya* **1989**, *3*, 23–25.
68. Ignatiev, V. V.; *et al.* Experience with alloys compatibility with fuel and coolant salts and their application to molten salt actinide recycler and transmuter. In *Proceedings of International Congress on Advances in Nuclear Power Plants*, Reno, NV, Jun 4–8, 2006.
69. Ignatiev, V. V.; *et al. Atom. Energy* **2006**, *101*(4), 278–285.
70. Ignatiev, V. V.; *et al. Nucl. Technol.* **2008**, *164*(1), 130–142.
71. Tripton, C. R. *The Reactor Handbook* **1960**, Vol. 3, p 464.
72. Litman, A. P.; *et al.* Corrosion associated with fluorination in the ORNL fluoride volatility process, ORNL-2832; ORNL: Oak Ridge, TN, 1961.
73. Hags, L.; *et al.* Comparative tests of L nickel, D nickel, Hastelloy B and INOR-1, ORNL-5924; ORNL: Oak Ridge: TN, 1968; pp 49–52.
74. Cavin, O. B.; *et al.* Molten salt reactor program semiannual report for period ending August 31, ORNL-4728; ORNL: Oak Ridge, TN, 1971; pp 173–176.
75. Bennett, M. R. Molten salt reactor program semiannual report for period ending February 29, ORNL-5132; ORNL: Oak Ridge, TN, 1976; p 170.
76. Counce, R. M. Molten salt reactor program semiannual report for period ending August 31, ORNL-5078; ORNL: Oak Ridge, TN, 1975; p 157.
77. Brown, C. H.; *et al.* Measurement of mass transfer coefficients in a mechanically agitated, nondispersing contactor operating with a molten mixture of $LiF–BeF_2–ThF_4$ and molten bismuth, ORNL-5143; ORNL: Oak Ridge, TN, 1976.
78. Savage, H. C.; *et al.* Engineering tests of metal transfer process for extraction of rare-earth fission products from a molten salt breeder reactor fuel salt, ORNL-5176; ORNL: Oak Ridge, TN, 1977.
79. Shimotake, H.; *et al. Trans. Am. Nucl. Soc.* **1967**, *10*, 141–142.
80. Siefert, J. W.; *et al. Corrosion* **1961**, *17*(10), 75–78.
81. Cavin, O. B.; *et al.* Molten salt reactor program semiannual report for period ending February 29, ORNL-4782; ORNL: Oak Ridge, TN, 1972; p 198.
82. Ingersoll, D. T.; *et al.* Status of preconceptual design of the advanced high-temperature reactor, ORNL/TM-2004/104; ORNL: Oak Ridge, TN, 2004.
83. Jordan, W. H.; *et al.* Aircraft nuclear propulsion project quarterly progress report for period ending June 10, ORNL-2106; ORNL: Oak Ridge, TN, 1956; p 95.
84. Jordan, W. H.; *et al.* Aircraft nuclear propulsion project quarterly progress report for period ending September 10, ORNL-2157; ORNL: Oak Ridge, TN, 1956; p 107.
85. Jordan, W. H.; *et al.* Aircraft nuclear propulsion project quarterly progress report for period ending December 31, ORNL-2221; ORNL: Oak Ridge, TN, 1956; p 125.
86. Jordan, W. H.; *et al.* Aircraft nuclear propulsion project quarterly progress report for period ending September 10, ORNL-2157; ORNL: Oak Ridge, TN, 1956; p 145.
87. Kondo, M.; *et al. Fusion Eng. Des.* **2009**, *84*(7–11), 1081–1085.
88. Olson, L. C.; *et al. J. Fluorine Chem.* **2009**, *130*, 62–73.
89. Keiser, J. R.; *et al.* The corrosion of type 316 stainless steel to Li_2BeF_4 ORNL/TM-5782; ORNL: Oak Ridge, TN, 1977.
90. Del Cul, G. D.; *et al.* Redox potential of novel electrochemical buffers useful for corrosion prevention in molten fluorides. In *Proceedings of the Thirteenth International Symposium on Molten Salts Held within the 201st Meeting of the Electrochemical Society*, Philadelphia, PA, May 12–17, 2002.
91. Brown, C.; *et al. Nucl. Eng.* **1994**, *35*(4), 122–128.
92. Konobeev, Y.; Birzhevoi, G. *Atom. Energy* **2004**, *96*(5), 365–373.
93. Generation IV Nuclear Energy Research Advisory Committee. Generation IV roadmap: Description of candidate liquid-metal-cooled reactor systems, GIF-017–00; Department of Energy: Washington DC, 2002.
94. Bakker, K.; *et al. Nucl. Technol.* **2004**, *146*, 325–331.
95. Susskind, H.; *et al.* Corrosion studies for a fused salt-liquid metal extraction process for the liquid metal fuel reactor, BNL-585; Brookhaven National Laboratory: Brookhaven, NY, 1960.